ISTANBUL TECHNICAL UNIVERSITY ★ GRADUATE SCHOOL

MIXED-ANION PHOTOCHROMIC YTTRIUM OXYHYDRIDE AND GADOLINIUM OXYHYDRIDE: RESEARCH AND APPLICATIONS

Ph.D. THESIS

Elbruz Murat BABA

Department of Nano Science and Nano Engineering

Nano Science and Nano Engineering Programme

FEBRUARY 2021

ISTANBUL TECHNICAL UNIVERSITY ★ GRADUATE SCHOOL

MIXED-ANION PHOTOCHROMIC YTTRIUM OXYHYDRIDE AND GADOLINIUM OXYHYDRIDE: RESEARCH AND APPLICATIONS

Ph.D. THESIS

Elbruz Murat BABA
(513152002)

Department of Nano Science and Nano Engineering

Nano Science and Nano Engineering Programme

Thesis Advisor: Prof. Dr. Esra ZAYİM
Thesis Co-Advisor: Dr. Habil., Ph.D. Smagul KARAZHANOV

FEBRUARY 2021

İSTANBUL TEKNİK ÜNİVERSİTESİ ★ LİSANSÜSTÜ EĞİTİM ENSTİTÜSÜ

KARIŞIK-ANYON FOTOKROMİK İTRİYUM OKSİHİDRAT VE GADOLİNYUM OKSİHİDRAT: ARAŞTIRMA VE UYGULAMALARI

DOKTORA TEZİ

Elbruz Murat BABA
(513152002)

Nano Bilim ve Nano Mühendislik Anabilim Dalı

Nano Bilim ve Nano Mühendislik Programı

Tez Danışmanı: Prof. Dr. Esra ZAYİM
Eş Danışman: Dr. Habil., Ph.D. Smagul KARAZHANOV

ŞUBAT 2021

M.Sc. Elbruz Murat Baba, a Ph.D. student of ITU Graduate School student ID 513152002, successfully defended the thesis/dissertation entitled "MIXED-ANION PHOTOCHROMIC YTTRIUM OXYHYDRIDE AND GADOLINIUM OXYHYDRIDE: RESEARCH AND APPLICATIONS", which he prepared after fulfilling the requirements specified in the associated legislations, before the jury whose signatures are below.

Thesis Advisor :	**Prof. Dr. Esra ZAYİM** İstanbul Technical University	.....
Co-advisor :	**Dr. Habil. Smagul KARAZHANOV** Institute for Energy Technology	.....
Jury Members :	**Prof. Dr. Nilgün YAVUZ** Istanbul Technical University	.....
	Assoc. Prof. Dr. Sevim İşçi TURUTOĞLU Istanbul Technical University	.....
	Dr. Mehmet Şeref SÖNMEZ Istanbul Technical University	.....
	Prof. Dr. Serap GÜNEŞ Yıldız Technical University	.....
	Assoc. Prof. Dr. Eda GOLDENBERG Sabanci University	.....

Date of Submission : 27 December 2020
Date of Defense : 04 February 2021

To my lovely spouse Aysima,

FOREWORD

This thesis would not be possible with the help and guidance from many people. I am where I am, because I stand on the shoulders of great people, two of whom I express my greatest gratitude however impossible; my mother Zühal and my father Süleyman.

I have been studying at Nano Science and Nano Engineering department from 2012 after completing an entirely unrelated field; Naval Architecture and Marine Engineering. I would like to thank, first, to my main supervisor including my MSc. studies, Prof. Dr. Esra ZAYİM, whose understanding and guidance helped my work in this thesis and earlier for the last 8 years. Thank you again accepting me into science.

I had started my journey in science by a motivation; improve the industry that deals with the largest, marine engineering, with remarkable advancements from science that deals with the smallest, nanoscience. Throughout this journey, transition from pure engineering to science in my master's studies was especially tough but nothing can hope to reach the exhilarating pace during my Ph.D. study. I have learnt a great deal during which again I was able to expand my knowledge and experience as an experimentalist. I present my gratitude for giving me this chance where I hope I have fulfilled; my co-supervisor Dr. Smagul KARAZHANOV. My efforts would have been pointless without the support you have given me during my Ph.D. studies.

I would also thank Dr. Jose Montero AMENEDO who has been a valuable unofficial adviser on my Ph.D., and I am delighted to call you my friend. I regret deeply we could not be able to work at the same group any more than we had!

I would like to give special thanks to my university, Istanbul Technical University, and staff for teaching me a completely new dimension during my master's and Ph.D. studies and paving the way towards a greater understanding.

Great deal of my work was carried out within the Solar Energy Department at the Institute for Energy Technology (IFE), and I would like to thank of all collegues, members and friends for contributing to my work in many ways. However, some people deserve special thanks. Åsmund, Anders, Bjørn, Heine, Anjitha, Guro, Nathan, Marte, Damir, Dmitry, Samson, Philip and many more, thank you for sharing great deal of conversations and being there for each other. I particularly thank Mari B.Ø. for showing such a bruléeist attitude, bringing joy and binding the group! I also thank to our engineers (Chang, Bent) and administrative members (Sean Erik, Erik, Arve) for keeping the department work like a clock.

After all, nothing I did could have been fun without you, Aysima. Thank you for putting up with my insufferable impatience.

December 2020

Elbruz Murat BABA
Naval Architect and Marine Engineer
Nano Scientist and Nano Engineer

TABLE OF CONTENTS

Page

ABBREVIATIONS

IGU	**:** Integrated glass unit
DC	**:** Direct current
UV	**:** Ultra-violet
ToF-ERDA	**:** Time-of-flight elastic recoil detection analysis
RBS	**:** Rutherford backscattering spectrometry
ERD	**:** Electron recoil detection
XPS	**:** X-ray photoelectron spectroscopy
XRD	**:** X-ray diffraction
LED	**:** Light-emitting diode
CA	**:** Contact angle
EG	**:** Ethylene glycol
MeI	**:** Methylene iodide
VASP	**:** Vienna abinitio simulation package
DFT	**:** Density functional theory
PAW	**:** Potential projector augmented wave
GGA	**:** Generalized gradient approximation
PBE	**:** Perdew Burke-Ernzerhof
HSE	**:** Heyd-Scuseria-Ernzerhof
AFM	**:** Atomic force microscopy
NMR	**:** Nuclear magnetic resonance
REMOH	**:** Rare-earth metal oxyhydrides
PAS	**:** Positron annihilation spectroscopy
GIXRD	**:** Grazing incident x-ray diffraction
JCPDS	**:** Joint Committee of powder Diffraction Standards
IR	**:** Infrared
CPD	**:** Contact potential difference
RH	: Relative humidity
SEM	: Scanning electron microscopy

SYMBOLS

K	**:** Kelvin
eV	**:** Electronvolt
nm	**:** Nanometer
GPa	**:** Gigapascal
YH_3	**:** Yttrium hydride
H	**:** Hydrogen
O	**:** Oxygen
YHO	**:** Yttrium oxyhydride
GdHO	**:** Gadolinium oxyhydride
PL	**:** Photoluminescence
Pd	**:** Palladium
T	**:** Transmittance
µl	**:** Microliter
θ_e	**:** Equilibrium contact angle
E_{cut}	**:** Energy cut-off
T_{lum}	**:** Luminous transmittance
Zr	**:** Zirconium
C	**:** Carbon
Y	**:** Yttrium
γ_{total}	**:** Total interfacial tension
γ^{LW}	**:** Lifshitz-van der Waals interaction
γ^{AB}	**:** Acid-base interaction
γ^{+}	**:** Lewis-acid
γ^{-}	**:** Lewis-base
mJ/m^2	**:** Milijoule per square meter
Å	**:** Ansgström
Pa	**:** Pascal
Ar	**:** Argon
GdH_2	**:** Gadolinium hydride
Gd_2O_3	**:** Gadolinium oxide

ΔT : Transmittance change / photochromic contrast

ΔR : Reflectance change

ΔA : Absorptance change

δ : Intensity parameter (XRD)

W/cm^2 : Watt per square centimeter

L : Grain size

K : Shape factor

λ : Wavelength

β : Peak broadening at half maximum

R : Reflectance

A : Absorptance

T_{clear} : Transmittance at clear state

T_{dark} : Transmittance at photodarkened state

A_{clear} : Absorptance at clear state

A_{dark} : Absorptance at photodarkened state

R_{clear} : Reflectance at clear state

R_{dark} : Reflectance at photodarkened state

mW : Miliwatt

α : Absorption coefficiency

d : Thickness

h : Planc constant

ν : Wave frequency

Eg : Energy of bandgap

MeV : Megaelectronvolt

E : Photon energy

P_d : Deposition pressure

CaF_2 : Calcium fluoride

InSb : Indium antimonide

ZnSe : Zinc selenide

i : Initial

f : final

OH : Hydroxide

AM1.5G : Solar spectrum air mass 1.5 global

TiO_2 : Titanium oxide

YBCO : Yttrium barium copper oxide

LaH **:** Lanthanum hydride

KOhm **:** Kiloohm

kV : Kilovolt

LIST OF TABLES

Page

LIST OF FIGURES

Page

MIXED-ANION PHOTOCHROMIC YTTRIUM OXYHYDRIDE AND GADOLINIUM OXYHYDRIDE: RESEARCH AND APPLICATIONS

SUMMARY

Rare-earth metal oxides and hydrides are the focal point in literature, promising various high demand solutions in industry and everyday life. Recently, a multi-functional, multi-anion material class called “rare-earth metal oxyhydrides” were shown to be synthesized as a thin film under ambient temperatures with photochromic properties. Oxyhydrides present high level of flexibility for material development through various combination possibilities having multi-anions. The newly realized possibility of ambient temperature thin film synthesis possibility of rare-earth metal oxyhydrides attracted high attention from literature but, there is little to no data is available in conventional databases for rare-earth oxyhydrides. Combination of the oxyhydrides being an under-developed class of materials and the promise of presenting important solutions for a high demanding era we live in, oxyhydrides is an excellent topic to research.

In 2011, the synthesis of yttrium hydride thin film in room temperature with wide-spectrum transparency using only one step deposition process was shown. Originally, this research started to search for an alternative material for solar cells but, evolved into another dimension when the material was realized to be a highly responsive photochromic material that can modulate in wide spectrum. The material attracted high attention from literature and initially named as “oxygen containing yttrium hydride”. However, it was later found through synchrotron measurements that this material is belong to the emerging class of materials; rare-earth metal oxyhydrides.

When exposed to air, yttrium dihydride (YH_2) and gadolinium dihydride (GdH_2) films turn into insulating and transparent yttrium oxyhydride (YHO) and gadolinium oxyhydride (GdHO), respectively. Oxidation in air, hence bandgap, can be controlled by deposition parameters. MHO (M; rare-earth metal) photodarkens when illuminated with light of adequate energy and intensity, recovers (bleaching) when stored in dark.

Photochromic rare-earth metal oxyhydride knowledge and know-how was established around synthesis method, band-gap engineering, optical properties, anion sites in the lattice etc. but the photochromic mechanism and environmental effects either yet to be understood or never even investigated before the present thesis work has been started. Also, yttrium was the only rare-earth element that was shown to have photochromic properties and investigated. Especially the knowledge gap over the interaction of photochromic oxyhydrides with the environment, prevented the realization into a product that sought heavily in industry. Therefore, in the present PhD thesis the interactions of the photochromic rare-earth metal oxyhydride thin films with the environment were first and foremost investigated. This endeavor resulted with solutions that enabled product development. Furthermore, contribution to the knowledge of photochromic rare-earth metal oxyhydrides by developing and studying at least one more rare-earth element next to the yttrium was also targeted.

The studies showed that photochromic rare-earth metal oxyhydride thin films interacts with environment heavily. Additionally, we have published one article in Physical Review Materials that tries to shine a light to the understanding of the rare-earth metal oxyhydride photochromic mechanism, related to the environmental interaction: "Light-induced breathing in photochromic yttrium oxyhydrides". The studies showed that during the photodarkening/bleaching cycle of yttrium oxyhydride, material releases/intakes oxygen following lattice contraction/expansion, respectively. We coined the term, *breathing*, after the accordion-like structural process of yttrium oxyhydride based on oxidation. The article was selected as an editor selection and featured in *Physics* magazine. Based on these studies, stable IGUs which has been long sought since 2016 was able to be manufactured.

Another contribution for the explanation of the photochromic mechanism of yttrium oxyhydride thin films published in Physica Status Solidi Rapid Research Letters with the title of "Temperature-dependent photochromic performance of yttrium oxyhydride thin films". In this article, we have presented the photochromic kinetics of yttrium oxyhydride thin films studied between 5-250K and presented a new approach which would enable new questions.

The second part of the PhD thesis plan was contributing to the knowledge of photochromic rare-earth metal oxyhydrides by at least one another rare-earth element. Gadolinium was selected as a member of the rare-earth elements for study for having similar chemical properties and widely accepted by the nuclear industry for large neutron capture diameter. In the span of a year, the production know-how and knowledge related to gadolinium oxyhydride thin films were elevated also. One article was published in the journal *Molecules* that shows the post-deposition oxidation is related with the preferential lattice orientation which controlled by the deposition parameters: "Preferential Orientation of Photochromic Gadolinium Oxyhydride Films". Additionally, another article based on the environmental interaction of gadolinium oxyhydride thin films will be submitted in an international journal in 2020.

Environmental effect on rare-earth metal oxyhydrides was investigated further by systematic study of yttrium oxyhydride thin films under atmospheres with varying relative humidity levels. Correlation between the relative humidity levels and photochromic kinetics was observed and microstructure formation that causes the delamination was shown. One article based on the results is under progress and planned to be submitted in 2021.

In the last part, applications developed during this thesis based on yttrium and gadolinium oxyhydride thin films were presented. First, photochromic kinetics of stable IGUs based on yttrium oxyhydride were presented. However, the properties photochromic rare-earth metal oxyhydrides present is much wider than only window applications as a result of their multi-anion nature. Lastly, photocatalytic properties of photochromic gadolinium oxyhydrides were also shown.

KARIŞIK-ANYON FOTOKROMİK İTRİYUM OKSİHİDRAT VE GADOLİNYUM OKSİHİDRAT: ARAŞTIRMA VE UYGULAMALARI

ÖZET

Nadir toprak metal oksitleri ve hidratları, son yıllarda insanlığın bir çok problemini çözmeye yönelik ürünlerin ortaya çıkmasına olanak sağlayan araştırmaların odak noktası olmaktadır. Bu grup elementler kullanılarak oldukça yakın bir zamanda, karışık-anyon yapılarına sahip nadir toprak metal oksihidrat ince filmlerin oda sıcaklığında ve tek kaplama basamağı ile üretilebildiği gösterilip fotokromik özellikleri keşfedilmiştir. Sahip oldukları karışık-anyon (oksit ve hidrit) yapısının sunduğu yüksek kombinasyon olanağı sayesinde, özgün malzeme geliştirilmesinde çok yüksek esneklik sağlanmaktadır. Fotokromik oksihidrat ince filmlerin oda sıcaklığında tek bir kaplama basamağı ile üretilebilme olanağı son yıllarda literatürden büyük bir ilgi görmüş olsa da, konvansiyonel malzeme bilgi merkezlerinde nadir toprak metal oksihidratları için bilgi bulmak neredeyse imkansızdır. Konvansiyonel malzeme bilgi merkezlerinde neredeyse hiç bilgi bulunamaması nadir toprak metal oksihidratlarının yeni olmasıyla beraber yüksek çeşitlilikte yeni malzeme üretilmesine olanak sağlayan karışık anyon yapıları sebebiyle ortaya çıkmaktadır. Tüm bu kısıtlı bilgi birikimi ve sahip olduğu ciddi sorunlara cevap üretebilme potansiyeli, üzerine çalışılmasını oldukça ilgi çekici kılmıştır.

2011 yılında yapılan çalışmalarla geniş spektrumda, yüksek ışık geçirgenlikli itriyum hidrat malzemelerin oda sıcaklığında üretilebildiği ilk defa gösterilmiştir. Fotovoltaik hücreler için malzeme geliştirmek üzere başlatılmış olan çalışma, malzemenin aynı zamanda hızlı tepki veren ve spektrumun tamamında optik modülasyon sağlayan fotokromik özelliğinin keşfedilmesiyle yeni bir boyut kazanmıştır. Literatürün hızlıca dikkatini çeken malzeme öncelikli olarak "oksijen içeren itriyum hidrat" olarak adlandırılsa da yapılan sinkrotron karakterizasyonları sonrasında malzemenin oksihidrat ailesine ait olduğu gösterildi.

İtriyum dihidrit (YH_2) ve gadolinium dihidrit (GdH_2) ince filmler hava içerisinde oksidasyon sonucu yalıtkan ve transparan yttrium oksihidrat (YHO) ve gadolinium oksihidrat'a (GdHO) dönüşmektedir. Kaplanan nadir toprak metal oksihidrat ince filmlerin hava içerisindeki oksidasyon ve dolayısıyla bant aralığı kaplama parametreleri ile kontrol edilebilmektedir. Elde edilen nadir toprak metal oksihidrat ince filmleri uygun enerji ve şiddete sahip ışık ile aydınlatıldığında kararıp ışık geçirgenliği geniş bir elektromanyetik spektrumda azalmakta, karanlıkta depolandığında ise transparan yapısına geri dönmektedir.

Fotokromik nadir toprak metal oksihidrat malzemeleri hakkında bilgi birikimi, bu tez çalışması öncesinde, üretim metodolojisi, bant aralığı mühendisliği, optik özellikler, kafes yapısı içerisindeki anyon konumları vb. konularda oluşturulmuş fakat, fotokromik mekanizma ve çevresel etkilerin malzeme davranışına etkisi henüz anlaşılamamış ya da üzerine hiç bir çalışma yapılmamıştır. Bununla beraber, bu tez çalışması öncesinde nadir toprak elementleri içerisinde sadece itriyum katyonu ile oksihidrat sentezine dair bilgi birikimi geliştirilmiştir. Çevresiyle etkileşimine dair

bilgi eksikliği, malzemelerin ürünleştirilmesinin önündeki en ciddi engellerden olmuştur. Bu sebeple, tez çalışmasına öncelikle malzemenin çevresiyle olan etkileşimi, özellikle ürün geliştirmeye engel olan etkileşimler, sonrasında ise uygulama geliştirme temelinde başlandı. Buna ek olarak, geliştirilen kaplama yöntem ve bilgisinin itriyum katyonuna ek olarak en az bir nadir toprak elementi üyesini daha ekleyerek genişletilmesi ikinci ana hedef olarak belirlendi.

Tez çalışması üç adet uluslarası dergilerde yayınlanmış makalelerin bir bütün hale getirilmesi ile oluşturulmuştur. Bu makalelerden ilki, *Physical Review Materials* dergisinde nadir toprak metal oksihidratlarının fotokromik mekanizmasının anlaşılmasına çevre ile etkileşim açısından katkı yapan, "Light-induced *breathing* in photochromic yttrium oxyhydrides" (Fotokromik itriyum oksihidratların ışık uyarımıyla *nefes alması*) başlığı altında 2020 yılında yayınlanmıştır. Çalışmalar, itriyum oksihidratın sırasıyla fotokromik kararma/ağarma çevrimi sırasında oksijen verip/aldığını ve bu çevrimi latis daralması/genişlemesinin izlediğini göstermiştir. Oksidasyon ile çalışan, akordiyon benzeri mekanizmayı temel alan "*nefes alan* (*breathing*)" terimi itriyum oksihidratın fotokromik çevrimi için ortaya atılmıştır. Çevre etkisine dayalı fotokromik çevrim sırasında itriyum oksihidrat ince filmlerinin yüzeylerinin hidrofobik özelliğinin kuvvetlendiği serbest yüzey enerjisi araştırmaları ile gösterilmiştir. Mor ötesi ışık altında tam tersi etki gösteren diğer fotoaktif ince filmler ile kıyaslandığında oldukça ilgi çeken ve çeşitli uygulama alanları doğurabilecek bir keşif olmuştur. Açığa çıkardığımız sonuçlar, teorik çalışmalar ile birleştirildiğinde, fotokromik nadir toprak metal oksihidratlarında oksijene bağlı ağarma bağıntısını göstererek nadir toprak metal oksihidratların fotokromik mekanizmasını açıklayan temel çalışmalardan biri olmuştur. Makale *Physical Review Materials* dergisi tarafından "editör seçimi" olarak seçilip *Physics* dergisi ana sayfasında ön plana çıkartılmıştır.

İtriyum oksihidratların çalışma mekanizması temelinde tez çalışması süresince yapılan bir diğer katkı "Temperature-dependent photochromic performance of yttrium oxyhydride thin films" (İtriyum oksihidrat ince filmlerin fotokromik performanslarının sıcaklık bağımlılığı) başlığı altında *Physica Status Solidi (RRL) Rapid Research Letters* dergisinde yayınlanmıştır. Bu çalışmada, itriyum oksihidrat ince filmlerin fotokromik kinetikleri 5-250 Kelvin aralığında kızıl ötesi spektrometri kullanarak incelenmiş ve fotokromik mekanizmanın işleyişine yeni bir yaklaşım getirilmiştir. Açığa çıkartılan sonuçlara göre, ultraviole ışık altında kararma etkisi itriyum oksihidrat ince filmin sıcaklığından bağımsız olarak gerçekleşmekte olup sıcaklığın filmin ağarma davranışına doğrudan etkisi olmaktadır. Ayrıca, itriyum oksihidrat ince filmlerinin farklı sıcaklıklarda gösterdiği değişken ağarma davranışı ağarma mekanizmasının iyon difüzyonuna ek olarak elektron difüzyonu da içerecek şekilde çok katmanlı ve kompleks olabileceğine işaret etmiştir.

Tez çalışmasının ikinci kısmı olarak, itriyum oksihidrat ile kısıtlı olan fotokromik oksihidrat literatürünü kimyasal özellikleri yakın kabul edilebilecek ve yüksek nötron yakalama çapı sebebiyle nükleer endüstrisinde yaygın olarak kullanılan gadolinyum ile genişletme amacı yer almaktadır. Bir senelik bir süre içerisinde, fotokromik gadolinium oksihidrat üretimi ve malzeme bilgi birikimi de geliştirilmiştir. Fotokromik gadolinyum oksihidrat üzerine yapılan çalışmalar "Preferential Orientation of Photochromic Gadolinium Oxyhydride Films" (Fotokromik gadolinyum oksihidrat filmlerinin tercihli kafes oryantasyonu) başlığı altında *Molecules* dergisinde yayınlanmıştır. Yayınlanan çalışmada, gadolinyum oksihidratların kaplama parametrelerine bağlı olarak tercihli kafes oryantasyonu

gösterdiğini ve taşlama sonrası oksidasyonun tercihli kafes oryantasyonu ile kontrol edilebileceği, bunun da fotokromik kinetiğini doğrudan etkilediği gösterilmiştir. Ayrıca, fotokromik gadolinyum oksihidrat sentezi sırasında oksidasyonun kontrolü sayesinde elde edilen filmlerin bant aralığının 1 eV düzeyinde değiştirilebildiği gösterilip aynı zamanda oksidasyonun kristal boyutu ile bağıntısı da ortaya konmuştur.

Tez çalışması içerisinde fotokromik itriyum oksihidrat ince filmlerin çevre ile olan etkileşimleri üzerine yapılan çalışmalar itriyum oksihidrat ince filmlerin saklandığı atmosferdeki nem sebebiyle bozunduğu gösterilmiştir. Çalışma içerisinde fotokromik kinetiğin nem oranına bağlı korelasyon gösterdiği saptanmış, tabandan yüzeye doğru oluşan mikro yüzey formasyonlarının nem ile etkileşime bağlı olarak bozunmaya sebep olduğu gözlenmiştir. Sonuçları bildiren bir makale henüz hazırlık aşamasında olup, 2021 içerisinde uluslarası bir dergide yayınlanması beklenmektedir.

Tezin son kısmında, yapılan çalışmalarla ulaşılan uygulama alanlarına dair sonuçlara yer verilmiştir. Tez süresince yapılan çalışmalar ile ulaşılan sonuçlar nadir toprak metal oksihidrat kaplamaların fotokromik yalıtkan camı olarak üretilmesine olanak sağlamıştır. Fotokromik itriyum oksihidrat yalıtkan cam ünitelerinin çalışma davranışıyla ilgili sonuçlar uygulama alanlarının öncüsü olarak yer almaktadır. Fotokromik nadir toprak metal oksihidratlarının çoklu-anyon yapısı ince film olarak oda sıcaklığında üretilebileceği gösterilmiş ve oldukça ilgi çekmiş olsa da sahip oldukları özellikler ve potansiyel fotokromik kaplamaların çok ötesindedir. Bu potansiyele ışık tutmaya yönelik sunulan ikinci uygulama alanı gadolinyum oksihidratların fotokatalitik davranışı ile ortaya konmuş ve tezin son kısmında ele alınmıştır.

1. INTRODUCTION

Photochromic oxyhydride materials received increasing interest since the first introduction of transparent yttrium hydride thin films prepared at room temperature [1] and photochromic properties [2] by Mongstad et. al. Photochromic thin films produced by rare-earth metals have been synthesized successfully by reactive magnetron sputtering [3] and e-beam evaporation [4]. Synthesis of rare-earth oxyhydride as bulk samples was also shown recently [5,6] by chemical method employing CaH_2 for anion substitution with lanthanide oxides. Moreover, the large flexibility of multi-anion compounds offer unique new material possibilities that single-anion materials cannot possess but, finding information for this emerging class of materials, rare-earth metal oxyhydrides, in conventional data bases is difficult or non-existent [7]. Synthesis of photochromic rare-earth metal oxyhydride consists of two steps: rare-earth metal hydride thin film deposition using reactive pulsed DC magnetron sputtering under argon and hydrogen atmosphere followed by the oxidation by exposing the film to air. Reactively deposited hydride layer is initially opaque rare-earth metal dihydride [3] which transitions into transparent after exposing to air resulting photochromic rare-earth metal oxyhydride (Figure 1.1). Resulting layer photodarkens when illuminated between UV and yellow light [8] and bleaches to its initial state when stored in dark.

Photochromism in yttrium hydride was first introduced by Ohmura et. al. [9] at GPa scale pressures and showing single phase of hexagonal-YH_3 show no optical change up to 10 GPa thus, indicating that coexistent state of multiple hydride phases might be important for photochromism. Later, Mongstad et. al. [1] demonstrated for the first time transparent yttrium hydride film deposition at room temperature with optical bandgap between 2.2 and 2.7, using pulsed DC reactive magnetron sputtering requiring no post deposition hydrogenation step and no palladium capping. Further, for the first time reversible photochromic properties of transparent yttrium hydride films was demonstrated [2] and the material named as ‘oxygen containing yttrium hydride’ with an oxide layer (5-10nm) on the surface [10] demonstrated by neutron reflectometry. It

was shown that the optical transmission and reflection can be modulated in a wide range, from UV to IR, by UV illumination. Also, electrical resistance decreases/increases up to a factor of 100 following darkening/bleaching, respectively. Photochromic mechanism studies of 'oxygen containing' yttrium hydride continued with Maehlen et. al. by demonstrating lattice contraction following photochromic response [11] using synchrotron x-ray diffraction (SR XRD) and suggesting that there may be a correlation between the two phenomena. Lattice contraction by photodarkening measurement through synchrotron study, which was also observed in XRD results [12], is important due to another study suggesting the contrary: photon-induced hydrogen transfer [13]. It was suggested that the photochromic mechanism is due to the photon-induced hydrogen transfer from hydrogenated oxide phase to hydride phase and the peak shift in XRD measurements is a result of changed in intensity. However, this mechanism is postulating an unlikely hydrogen loading into the oxide layer at ambient temperature, diffused from hydride phase, during bleaching when the photochromic "oxygen containing rare-earth hydride" thin film kept in dark in order to demonstrate the widely known photochromic reversibility of photochromic rare-earth oxyhydrides in a relatively rapid pace [14]. However, rehydrogenation process cannot take place at ambient pressure [15] which makes the process suggested by this theory irreversible.

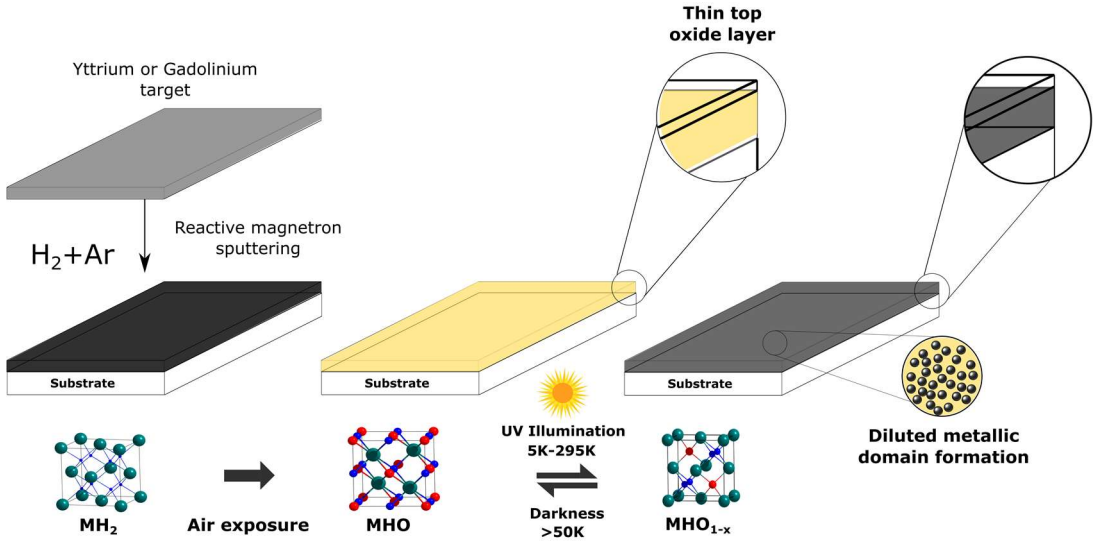

Figure 1.1 : Schematic representation of photochromic rare-earth metal oxyhydride synthesis and photochromic cycle.

On the other hand, if oxidation should take place after hydrogen anion diffusion during bleaching according to the suggested process [13], then it would also contradict the

photochromic reversibility of rare-earth metal oxyhydrides as a result of eventual full oxidation of the material.

Synchrotron study of photochromic yttrium hydride [11] is also important for suggesting for the first time the rearrangement of H and O atoms in the lattice could be involved for material synthesis. Photochromic mechanism of rare-earth metal oxyhydrides eluded scientists for a long time and several complex characterization methods were employed to reveal this intricate problem. Chandran et. al. utilized nuclear magnetic resonance (NMR) spectroscopy and observed loss in mobility of YH moieties under white light illumination and return of mobility after several days, suggested the release of electrons and metallic phase formation for photochromic mechanism [16]. However, they stated this effect can be a result of lattice distortion and not related or a cause for photochromic effect. Also, prior to the NMR study, oxygen concentration for photochromic films was unknown thus, role of oxygen was completely excluded from any conclusion. Even though this mobility change was pointed as a proof of a connection between unique photochromic mechanism and hydrogen anion; more studies on better controlled samples are needed to explain photochromic mechanism because of the "presence of many possible reasons for disappearance of the sharp spectral features" and the complete exclusion of the other key anion, oxygen [16]. Following, another promising study [17] that shines light on the photochromic mechanism of 'oxygen containing' yttrium hydrides was conducted by XRD and Raman characterizations using samples demonstrating the photochromic mechanism involves formation of highly diluted metallic domain formation. Through Maxwell-Garnett approximation it was shown that only 2% in volume of the metallic phase growth under illumination may cause more than 30% contrast in the visible region [17]. Metallic domain formation study created questions as much as it answered, such as the role of oxygen and the reason behind the reversibility of photodarkening.

Control over photochromic response is extremely important for applications and one of the key factors standing before device designs. You et. al. [18] demonstrated straightforward control over optical properties of 'oxygen containing' yttrium hydrides by changing deposition pressure by reporting direct bandgap change between 2.8-3.7 eV. It was argued in the study that this change might be the result of oxygen incorporation increase but no compositional study was provided until the following

study [19] where the effect of change in oxygen and hydrogen concentrations over optical properties was systematically investigated. It was presented that the black opaque 'oxygen-containing' yttrium hydride film can be transformed to a photochromic yellow transparent material when the oxygen concentration increased above a certain threshold. This result also proved an earlier work [3] that showed the initial deposition was opaque yttrium dihydride (YH_2) through investigation by aluminum capping as deposited yttrium hydride thin films without breaking the vacuum. The slow reaction with air, permitted by the porous aluminum capping layer, transformed the hydride layer into photochromic transparent 'oxygen-containing' yttrium hydride. During this transformation XRD measurements showed the peak transformation from dihydride to lower angles, indicating lattice expansion, as the thin film oxidized. Later, refractive index was calculated through ellipsometry studies [14] where only change was observed for the imaginary part k as increased during illumination. Also, the thickness dependence of photochromic contrast of "oxygen containing" yttrium hydride thin films were shown for the first time in the same study [14] by demonstrating higher thickness results with larger contrasts. Further spectrophotometry studies found that "oxygen-containing" yttrium hydride thin films presents an indirect allowed band gap between 2.5 and 2.6 eV but higher energy values for bandgap can be obtained between 3.2 and 3.3 eV if a direct allowed transition is considered [20]. In the same study, photoluminescence (PL) properties were also investigated and found that the PL yield is extremely low in transparent state and even lower in photodarkened state [20]. Later, thickness dependence was investigated further and shown that the photochromic response has a bulk nature [21]. Photochromic response can be controlled not solely by synthesis but also by illumination temperature and density. It was shown [8] that photochromic response of YHO thin films can be observed by illumination from UV (3.14 eV) to yellow light (2.20 eV) with intensities of 5.1 and 4.9 mW/cm^2, respectively. Photochromic response reduction was observed as the photon energy reduces towards yellow light. In the same study, it was also found that higher temperatures work against the photodarkening; higher the temperature is lower the photochromic response. Temperature and light intensity effect on photochromic response was also reported in an early thesis study [22].

After the demonstration of photochromic 'oxygen-containing' yttrium hydride is actually belong to yttrium oxyhydride (YHO) [23] by showing oxygen and hydrogen anions resides the tetrahedral sites through synchrotron measurements, name was adopted by the scientific community [24–28] and expanded to other rare-earth metal (Gd, Dy and Er) oxyhydrides with photochromic properties [24]. Showing photochromic properties by other rare-earth elements is especially important that demonstrates the great possibility and even larger flexibility of rare-earth metal oxyhydrides. After studying the composition of photochromic yttrium oxyhydride films using Rutherford backscattering spectrometry (RBS) and time-of-flight energy elastic recoil detection analysis (ToF-E ERDA), gradual oxidation was shown in samples following a decrease in hydrogen content [29], supporting You et. al. study [18]. Chemical formula derived from the compositional analysis was the next important step for investigating this emerging class of materials. Moldarev et. al. [26] performed a compositional analysis for YHO by utilizing time-of-flight elastic recoil detection analysis (ToF-ERDA) and revealed that oxygen replaces the hydrogen during oxidation, validating an earlier study [11] further by a powerful characterization method. As a result, a chemical formula was suggested for yttrium oxyhydride: $YH_{2-\delta}O_{\delta}$, $0.45<\delta<1.5$ [26]. In a parallel work [28], another chemical formula was also suggested using Rutherford backscattering spectrometry (RBS) and electron recoil detection (ERD); $MH_{3-x}O_x$, $0.5\leq x\leq 1.5$ where M represents rare-earth metal. According to the formula, each H atom can be replaced be one O. However, valance charge states of O and H are different and upon incorporating one O to Y, 2 H is expected to be released from Y cation. Chemical formula, $YH_{3-x}O_x$, of the yttrium oxyhydride was first predicted in an earlier theoretical article [30].

The results of the present PhD thesis have been documented in 3 papers published in international journals and disseminated in 4 international conferences as 4 invited talk and one oral presentations. One more paper to be published in an international journal is under progress.

Thesis research attention was focused on the following question: photochromic mechanism of rare-earth metal oxyhydrides. First approach was the investigation of photodarkening/bleaching mechanism that we have found should be approached separately and we have investigated in different atmospheric compositions; in N_2 and air [12]. In the first paper presented in this thesis, we have demonstrated the

atmospheric effect on photochromic YHO and the bleaching dependency over oxidation. The mechanism has led us study the surface further by XPS and wettability investigations using tensiometer. Moreover, structural characterizations revealed interesting results that we coined the term for the behavior of photochromic oxyhydride photodarkening/recovery cycle as "*breathing*". Combined with the theoretical investigations, we showed the dependency of rare-earth oxyhydrides photochromic reversibility on environment [12] for the first time, specifically oxidation, that underpins the photochromic mechanism. Following this finding, we have investigated and presented as a second study in this thesis the resulting effect by environment and possible control during oxidation just after the magnetron sputtering with another photochromic oxyhydride; gadolinium oxyhydride (GdHO) [31]. We uncovered the influence of deposition parameters and film composition on oxidation resulting with varying levels of photochromic performance as well as bandgap. This study was the second investigation showing the environmental effect during synthesis controlled by the deposition parameters. We have investigated the environment effect over rare-earth metal oxyhydrides further and found that the water content in air have an adverse effect on yttrium oxyhydrides; yttrium oxyhydride thin film delamination. We have shown the correlation between relative humidity levels on photochromic kinetics and formation of microscopic features that causes delamination. Third and last published study demonstrates the investigation of YHO thin films using IR spectroscopy. It was shown that photochromic performance is dramatically influenced by temperature [32]. We have uncovered insightful results between temperature ranges of 5-250 K. This study was important by showing photodarkening and recovery might be governed by different mechanisms other than solely by anion transport. As the last part of this thesis, three different application results were presented: photochromic integrated glass unit (IGU) with yttrium oxyhydride, photocatalysis and superconductivity by gadolinium oxyhydride. This thesis is a small but sure step showing how large the rare-earth oxyhydride potential is and, only the surface has been revealed yet.

2. LIGHT-INDUCED BREATHING IN PHOTOCHROMIC YTTRIUM OXYHYDRIDES[1]

2.1 Introduction

Yttrium hydride and other rare earth hydrides are extremely strong reducing agents, a feature that complicates considerably their study. For their adequate handling in air, rare earth hydride thin films are usually protected against oxidation by, for example, Pd capping layers [15]. However, the incorporation of oxygen in rare earth hydrides after intentional exposure to air [3,24,25], or even through accidental contamination [33], leads to the formation of oxyhydrides, materials that contain oxide and negatively charged hydride [7,28,34,35], which exhibit very interesting properties. One of the pioneering works on this family of materials was carried out by Miniotas et al. [33], who reported gigantic electrical resistivity in oxygen-containing gadolinium hydride. Later, Mongstad et al. [2] reported photochromic properties in oxygen containing yttrium hydride, a feature observed very recently by Nafezarefi et al. [24] in other rare earth oxyhydrides such as dysprosium, gadolinium or erbium oxyhydrides. The photochromism in Y-related compounds can be traced back to Ohmura et. al [9], who observed light induced reversible darkening in yttrium hydride thin films subjected to high pressures (≈GPa). Despite the importance of the discovery, the emergence of this new inorganic photochromic material went unnoticed at that time, presumably because the pressure range required is not suitable for practical applications. Today, however, it is known that yttrium oxyhydride as well as other rare earth oxyhydrides, are photochromic at room temperature and at ambient pressure; hence, YHO, as an inorganic photochromic material has multitude of potential applications [36]. Note that in the text we refer to yttrium oxyhydride simply as YHO, a notation that, in principle, is not related to the stoichiometry of the compound, which will be discussed later. The origin of the photochromic mechanism in YHO is still open to debate and has been

[1] This chapter is based on the paper: Baba, E. M., Montero, J., Strugovshchikov, E., Zayim, E. Ö., Karazhanov, S. (2020). Light-induced breathing in photochromic yttrium oxyhydrides. *Physical Review Materials,* 4, 025201. https://doi.org/10.1103/PhysRevMaterials.4.025201 - Creative Commons Attribution 4.0 International license

attributed to different causes [16,17,37]. In the present paper, the study of the wettability of the YHO surface under illumination and darkness conditions, as well as the photochromic darkening/bleaching dynamics in air and in inert atmosphere, unraveled the cause that underpins the photochromism in YHO. According to our observations, oxygen diffusion takes place during illumination (in consequence the YHO lattice contracts). The displaced oxygen atoms leave behind an oxygen-deficient structure responsible for the optical darkening, which is in agreement with our previous observations [17]. In darkness, the YHO lattice expands back because of the filling of the oxygen vacancies by oxygen atoms, allowing the film to bleach back to its original state. Since YHO expands/contracts reversibly under dark/illumination cycling produced by the displacement inwards/outwards of oxygen atoms, we refer to this process as breathing. Due to this breathing, the correct bleaching of the photo-darkened YHO coatings depends on the availability of an oxygen source. Thanks to the light-induced oxygen diffusion, YHO could be used for other purposes such as sensing and optical memories, broadening the traditional fields of application of photochromic materials.

The wettability of YHO under illumination is unusual. All oxides and nitrides of low-electronegativity metals can exhibit hydrophobicity [38,39]. It can be, therefore, expected that YHO exhibits hydrophobic properties as well. However, while the surface of yttrium oxyhydride increases its hydrophobicity when illuminated, other metal oxides turn into hydrophilic under UV illumination. In the latter case, the formation of electron-hole pairs under illumination leads to the creation of defect sites, where hydroxyl groups can be adsorbed, leading to hydrophilic properties [40]. Generally, when metal oxides are stored in darkness during periods of time ranging from 7 to 50 days [41,42], oxygen replaces back the adsorbed hydroxyl groups, giving raise to hydrophobicity. In the present work, the unexpected behavior observed in YHO, i.e., the enhancement of the hydrophobic properties under illumination, has been found to be caused by the same reason, that is, the oxygen-enrichment of the surface under illumination.

2.2 Methods

YHO thin films were prepared onto glass substrates following a two-step deposition process. First YH_2 metallic films were fabricated by magnetron sputtering in a Leybold

Optics A550V7 sputter unit. Second, postdeposition oxidation in air transformed YH_2 to YHO. In order to achieve YHO upon air exposure, precursor YH_2 films have to be deposited when the chamber pressure is above a certain critical value, which results in films with large structural disorder [27]. Further details on the synthesis process of photochromic YHO can be found elsewhere [3,14,27]. A cold white LED array from Thorlabs (colour temperature 4600-9000 K) was used as illumination source for the photo-darkening experiments. The crystallographic structure of the obtained films was characterized by using x-ray diffraction (XRD) in a Bruker Siemens D500 spectrophotometer (CuKα radiation, parallel beam geometry). The composition and surface oxidation states were studied by Xray photoelectron spectroscopy (XPS) in an Ulvac PHI Quantera II instrument. Surface roughness characterizations were performed using atomic force microscopy with area of 5 μm^2 from Photonic Technologies picostation. The optical transmittance (T) of the YHO films in the clear and photodarkened state was measured using an Ocean Optics spectrophotometer QE65000 and a Perkin-ElmerLambda-900 with integrating sphere. Contact angle (CA) measurements were performed using KSV Attension Optical Tensiometer under air. 5 µl drop volume was used for each CA measurement and three different sessile droplets were measured on several substrates for each value and averaged with a standard deviation of ±2. CA values in the equilibrium (θ_e) for water, ethylene glycol (EG), and methylene iodide (MeI)–both EG and MeI from Sigma-Aldrich–were used to calculate surface free energies of yttrium oxyhydride films at clear and photo-darkened state using the van Oss-Good-Chaudhury method [43,44].

The calculations were performed with the Vienna Abinitio Simulation Package (VASP) code [45–47], based on density functional theory (DFT) using a plane-wave pseudopotential method together with the potential projector augmented-wave (PAW) [48–50]. The generalized gradient approximation (GGA) in the scheme of Perdew Burke-Ernzerhof (PBE) is used to describe the exchange correlation functional [47]. To describe the electron-ion interaction standard PAW-PBE pseudopotentials [51] are used with $1s^1$ for H, $2s^2 2p^4$ for O and $4s^2 4p^6 4d$ for Y atoms as the valence-electron configuration. The plane wave functions of valence electrons are expanded in a plane wave basis set, and the use of PAW pseudopotentials allows a plane wave energy cutoff (E_{cut}). Only plane waves with kinetic energies smaller than E_{cut} are used in the expansion. Reciprocal-space integration over the Brillouin zone is approximated

through a careful sampling at finite number of k-points using a Monkhorst-Pack mesh [50]. We choose the energy cutoff to be 700 eV, and the Brillouin-zone sampling mesh parameters for the k-points set are 8 x 8 x 8. In the optimization process the energy change is set to 1 x 10^{-6} eV. The charge densities are converged to 1 x 10^{-6} eV in the self-consistent calculation. The range-separated hybrid Heyd-Scuseria-Ernzerhof (HSE06) functional is used for density of states calculations [52,53]. The hybrid functional requires a standard value of the (short-range) Hartree-Fock exchange (21%) mixed with a portion of PBE exchange (79%), also known as the HSE06 hybrid functional [53,54]. Selection of the parameter has been performed as an inverse value of infinity dielectric constant that is valid, if the energy band gap of these systems is larger than 3 eV.

2.3 Results and Discussion

2.3.1 Hydrophobicity control through light illumination

YHO thin films exhibit photochromic properties, that is, YHO films undergo a reversible decrease of their optical transmittance when illuminated with light of adequate energy and intensity [14]. Figure 2.1 shows the transmittance in the clear and photodarkened state for a 1400-nm-thick YHO film. This film decreased its luminous transmittance T_{lum} [55] from 78.5% to 26.7% after illumination. The luminous efficiency of the human eye (photopic vision) is presented in Figure 2.1(a) for comparison [55] . How to obtain such optical contrast by illumination will be discussed in detail in the next section. Recent studies by Nafezarefi et al. [27] revealed that the bleaching dynamics and photochromic contrast in YHO is affected by Zr doping.

Nonilluminated (clear) YHO thin films show hydrophobicity with equilibrium contact angle θ_e values of 95° for water (see Table 2.1); however, θ_e values increased to 115° after illumination (again in the case of water), see Table 2.1 and Figure 2.1(b). Table 2.1 also shows θ_e for ethylene glycol EG and methylene iodine MeI for the clear and photodarkened states. In the case of MeI, θe also increases after illumination, from 43°, yet remains constant for EG. Atomic force microscope AFM studies performed in such films revealed a relatively smooth surface with a rms value of surface roughness of around 8 nm.

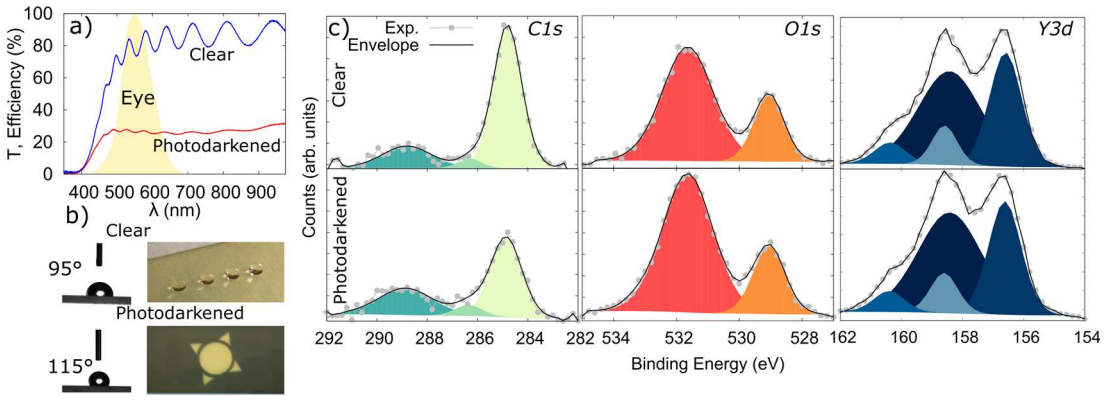

Figure 2.1 : Different properties measured in the clear state and photodarkened state (after illumination) for a 1400-nm-thick YHO film: transmittance compared to the luminous efficiency of the human eye in photopic vision [panel (a)], contact angle photographs for water, a photo of water droplets onto a clear film, as well as the same film after being illuminated under a sun-shaped mask during1h [panel(b)]. XPS spectra corresponding to C1s, O1s and, Y3d [panel (c)].

The observed initial hydrophobicity of the YHO films (clear state) can be explained by the electronic structure of rare-earth elements. According to a detailed experimental analysis of the entire rare-earth oxide series carried out by Azimi et al. [39], the unfilled 4f orbitals shielded by a full octet of electrons from the $5s^2p^6$ shell result in a lower tendency of such compounds to form hydrogen bonds with the adjacent water molecules [39,56]. Hydrophobicity is not exclusive of the lanthanide f-shell group, but it can be achievable in any metal oxide provided that the electronegativity of such metal is low enough [38]. The low electronegativity of Y and the prevalence of yttrium oxide at the surface [29] explains the high θ shown inTable 2.1.

One might expect decreased hydrophobicity under illumination caused by electron-hole pairs. Such behavior occurs in other metal oxides [40,41,57–60]. As we stated previously, however, hydrophobicity in YHO is enhanced under illumination. The light-induced decrease of wettability can be explained through changes in the oxygen-to-metal ratio at the surface. In metal oxides, coordinatively unsaturated oxygen atoms work as a Lewis base while the metal cations work as Lewis acid. Combined Lewis acid and base orientation of the surface causes high affinity towards water molecules [61], therefore the oxygen-to-metal ratio in the surface is crucial for understanding the wettability properties [62].

Table 2.1 : Equilibrium contact angle values (θ_e) for water, ethylene glycol (EG), and methylene iodine (MeI), as well as the measured total surface energy (γ_{total}) and its components: Lifshitz–van der Waals interactions term (γ^{LW}) and acid-base interaction term (γ^{AB}) calculated from the Lewis acid and base parameters ($\gamma+$ and $\gamma-$, respectively). All data given for the clear and photodarkened state.

	θe (Water) (deg)	θe (EG) (deg)	θe (MeI) (deg)	γ_{total} (mJ/m^2)	γ^{LW} (mJ/m^2)	γ^{AB} (mJ/m^2)	γ^{+} (mJ/m^2)	γ^{-} (mJ/m^2)
Clear state	95	81	43	45.55	38.07	8.98	2.98	6.76
Photodarkened state	115	81	60	28.88	28.58	0.31	0.18	0.13

In order to study the compositional changes of the YHO surface, XPS measurements were performed before and after illumination. The results are presented for C1s, O1s, and Y3d in Figure 2.1(c). See Table 2.2 for the quantification of the different elements by XPS. The quantification has been done using survey spectra (not shown) considering Y3s, O1s, and C1s (column A) or Y3p, O1s, and C1s (column B) for both the clear and dark state.

The carbon (adventitious) C1s signal can be deconvoluted into three different contributions. The signal corresponding to C-C has been established at 284.8 eV as a charge correction reference. Other contributions are located at 286.3 eV attributed to C-O-C and/or C-OH, which are expected to present a 1.0 eV difference in energy and hence are difficult to resolve), and O-C = O at 288.8 eV [63].

After illumination, the carbon content on the surface decreases, see Table 2.2. This decrease is more pronounced in the C-C contribution, Figure 2.1(c). Since the content of C in the surface decreases, the increase of adsorbed hydrocarbons is ruled out as the possible cause for the light-induced enhancement of the hydrophobicity [64–66]. Nevertheless, a decrease in carbon content can result in an increase of the intensity of the XPS contributions located at higher energies [67]. In particular, the decrease of carbon may result in an increase of the O1s intensity when compared to the intensity of the Y3d signal. For this reason, O/Y ratios in Table 2.2 have been calculated using Y3s and Y3p levels, which are closer in energy to O1s than Y3d.

Table 2.2 : Quantification by XPS of the O, Y, and C content at the surface of a yttrium oxyhydride film in the clear and photodarkened state. Two sets of data are presented in each case. In case A the quantification has been done, taking into account levels C1s, O1s, and Y3s, whereas in B, O1s, C1s, and Y3p were considered instead.

	Clear State		**Dark State**	
	A	**B**	**A**	**B**
C (at %)	45.6	47.0	35.8	36.7
O (at %)	38.4	37.9	48.1	46.9
Y (at %)	16.0	15.2	16.2	16.4
O/Y	2.4	2.5	3.0	2.9
C/Y	2.9	3.1	2.2	2.2

The O1s signal is composed of two contributions at 529.0 and 531.2 eV. The former can be attributed to O atoms bound to Y atoms, whereas the latter can be assigned to atomic oxygen [68]. After illumination, the oxygen-to-yttrium atomic ratio of the surface increases, see Table 2.2. This increase is consistent when comparing the O1s level to Y3s and Y3p levels, and takes place both for O bound to Y as well as for atomic O. The largest increase is observed in the latter, Figure 2.1(c). The contributions of the carbonates in the O1s region seem to be negligible.

The obtained results for Y3d correspond very well to the Y_2O_3 stoichiometry. At the surface the samples consist of Y_2O_3, which agrees with our previous work [29]. The Y3d has well-resolved spin-orbit components, namely, Y3d and $Y3d_{5/2}$. These components can be deconvoluted into Y_2O_3, with contributions at 156.6 and 158.4 eV, Figure 2.1(c) [68]. An extra doublet is needed for completing the fitting, with contributions at 158.6 and 160.3 eV. In this energy range, the possibilities are Y-OH [69], yttrium carbonates [69], and Y-H [70], the latter being the best candidate, since no evidence of carbonates and hydroxides is found in C1s or O1s. There is not a remarkable change in Y3d before and after illumination.

When comparing the current XPS results with previous published data [71], it is evident that the films studied here, obtained by an optimized sputtering process [3], present higher homogeneity.

Surface-energy calculations, performed using the van Oss–Chaudhury–Good method [43,44], confirm the lower wettability through reduction under illumination of the total surface energy γ_{total}, see Table 2.1. The enrichment in oxygen of the surface, confirmed by XPS, reduces the Lewis sites as the surface approaches the Y_2O_3 stoichiometry. The nonpolar Lifshitz–van der Waals surface-energy component γ^{LW} also decreases from 38.07 to 28.57 mJ/m^2, while the polar acid-base component γ^{AB} decreases from 8.98 to 0.31 mJ/m^2 after illumination. Here $\gamma^{AB} = 2(\gamma^+\gamma^-)^{1/2}$, where γ^+ is the Lewis acid and γ^- the Lewis base parameters of surface tension.

Hydrophobic yttrium-based oxides have been reported in the past [38,72]. In those works, as Y_2O_{3-x} coatings approached Y_2O_3 stoichiometries, contact angles increased [72]. This pattern is consistent with metal-to-oxygen ratios of surface studies [62]. Consequently, the enrichment in oxygen of the surface under illumination causes the light-induced hydrophobicity enhancement observed in YHO thin films. In the next section, the exchange of oxygen atoms between the film and the atmosphere, induced by illumination, is demonstrated.

2.3.2 Light-induced *breathing*

Photochromic yttrium oxyhydride has been obtained by the oxidation in air of reactively sputtered metallic YH_2 films. The effect that the ambient humidity plays in this transformation is unclear. The incorporation of oxygen in the YH_2 lattice causes the increase of the lattice constant *a* from 5.20 to 5.34 Å [1,3,24] and hence the displacement of the diffraction peaks towards lower angles. Under illumination, the lattice of the YHO films contracts back, but without reaching the original oxygen-free YH_2 lattice constant [11].

After the incorporation of oxygen, NMR studies revealed that most of the hydrogen atoms in YHO remained in a local environment very similar to tetrahedral positions in YH_2 [16]. Small signals, which can be attributed to mobile protons and to oxygen coordination, arise as well after air exposure.

Figure 2.2(a) shows a grazing incidence XRD pattern corresponding to a yttrium oxyhydride sample in its initial (clear), illuminated (photodarkened), and recovered

(bleached) state. The standard diffraction peaks for YH_2 and Y are also shown for comparison [Joint Committee of Powder Diffraction Standards (JCPDS) Cards No. 04-002-6938 and No. 04002-7545].

The analysis of the XRD patterns revealed how the films undergo an accordionlike transformation: the YHO lattice contracts and expands when subjected to illumination/darkness cycles.

Our previous optical studies pointed to the reversible formation of oxygen-deficient YHO metallic domains [17] within the dielectric YHO_{1-x} lattice as the cause of the photochromic behavior and lattice expansion/contraction:

$$YHO \underset{darkness}{\overset{illumination}{\rightleftharpoons}} (1-\eta)\mathrm{YHO}+\eta YHO_{1-x} + \eta xO \tag{2.1}$$

Since the filling factor ff of the YHO_{1-x} domains is predicted to be very small [17], the factor η must be $\eta << 1$. Dilution of YHO_{1-x} domains in the dielectric YHO structure is necessary to achieve higher optical absorption rather than higher optical reflectance, which is consistent with experimental observations [2,14].

Very few oxygen atoms need to be released under illumination to produce a large optical contrast. In fact, $ff = 0.02$ causes a drop of the visible transmittance larger than 30% [14]. In addition, not all the released oxygen atoms necessarily need to leave the sample, and the material is able to host the outdiffused O atoms [73]. This was confirmed also by XPS in Fig. 2.1(c). Therefore, although the effective medium approximation works very well for modeling the optical properties [14], it is very difficult to confirm the release of oxygen in the experiment.

However, we postulate that there must be some exchange of oxygen atoms under illumination/darkness between the sample and its surroundings. This exchange, as discussed before, is probably below the detection limit of most conventional techniques. To prove our hypothesis, YHO thin films were subjected to 2h period cycles (0.5 h illumination followed by 1.5 h darkness) inside a glovebox filled with N_2 and H_2O content within the glovebox was below 0.1 and 1.4 ppm, respectively. The average transmittance of the film was measured between 600 and 800 nm during cycling and plotted in Figure 2.2(b). In the absence of air, the films lost part of their initial transparency in each cycle, not being able to recover fully. After 4 weeks of continuous cycling within the glovebox, the luminous transmittance Tlum of the

samples decreased from 78.5% in the nonilluminated state to 26.7%. This heavily photodarkened films were allowed to bleach in total darkness, both in air and in N_2 atmosphere (glovebox). The evolution of T_{lum} is presented in Figure 2.2(c). The bleaching speed of the photodarkened samples in darkness was much slower inside the glovebox than in air. In addition, during the recovery, a series of transmittance measurements were performed during a period of 24 h, both in air [Figure 2.2(d)] and in the glovebox [N_2 atmosphere, Figure 2.2(d)].

The films kept in air recover their initial transparency after a few hours [T_{lum} clear, presented in Figure 2.2(c) as a horizontal dashed line], while the films in N_2 recovered very little in the same period of time. Since there are no significant differences between the temperature inside and outside of the glovebox (both at ~20◦C), the data presented in Figure 2.2(c)–(e) strongly indicate that a source oxygen from the ambient is crucial for adequate recovering of the photodarkened films. The need for ambient oxygen, and possibly water vapor, is consistent with the light-induced oxygen release hypothesis summarized in Equation (2.1).

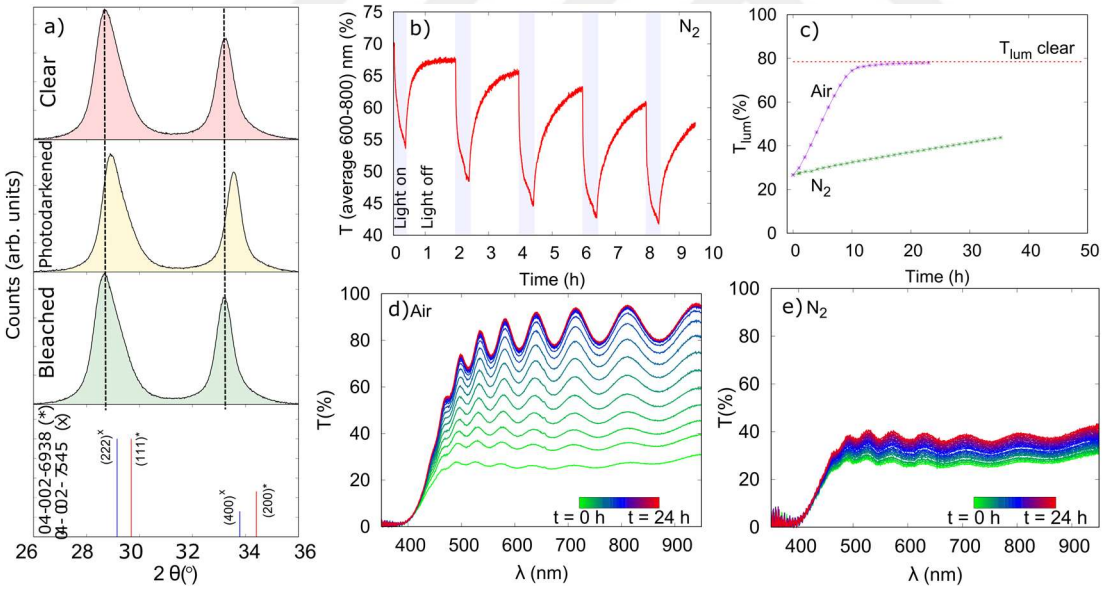

Figure 2.2 : Structural and optical changes under light illumination and the dependence of the photochromic dynamics on the atmosphere: x-ray diffraction patterns for a 1400-nm-thick YHO sample at the initial, dark, and bleached state [panel (a)]. Average transmittance measured between 600 and 800 nm during 0.5-h illumination followed by 1-h darkness in a sample kept in N2 atmosphere [panel (b)]. Differences in the recovery dynamics for the sample kept in air vs the sample kept in N2 atmosphere, as illustrated by the measurement of the luminous transmittance Tlum vs time [panel (c)] and by a series of transmittance measurements vs time [panels (d) and (e)].

The dependence on the atmospheric composition rules out other possible explanations for the photochromic mechanism, including light-induced formation of defect pairs or lattice distortion [16]. The release of hydrogen [37] (instead of oxygen) is an alternative explanation that can also be ruled out but for a different reason. In this case, the reversibility of the process would require the rehydrogenation of the film, a process that cannot take place at ambient pressure [15]. Nevertheless, if hydrogen is released, the film could bleach by the incorporation of O, eventually approaching the Y_2O_3 stoichiometry. However, this hypothesis is not supported by the x-ray diffractograms shown in Figure 2.2(a) and contradicts the reversibility of the process. Besides, the very large band gap of Y_2O_3 would lead to an increase of T_{lum}. Such increments are not observed, Figure 2.2(c) and (d).

Considering the low electronegativity of Y, the idea of oxygen being pushed out of the YHO lattice by illumination may seem counterintuitive at first. The thermodynamics and kinetics of Eq. (2.1) need further studies for clarification. In the next section, a preliminary theoretical model for understanding the light-induced oxygen release in YHO films is presented.

2.3.3 Theoretical considerations

The experimental evidence presented above points to light-induced oxygen exchange between the film and the atmosphere. In the present section, this question is addressed by DFT modeling (ab initio calculations using VASP 5.3.5). It is known that photochromic YHO coatings are obtained experimentally by the partial oxidation of YH_2 films in air. As discussed before, the incorporation of oxygen into YH_2 results in the expansion of the YH_2 lattice. The lattice parameter *a* increases, and hence the XRD peaks corresponding to YHO appear displaced towards lower angles when compared to oxygen-free YH_2, Figure 2.3(a). The data presented in Figure 2.3(a) corresponds to two different samples. The evolution of the XRD pattern for the same sample before, during, and after the YH_2-to-YHO transformation can be found elsewhere [3].

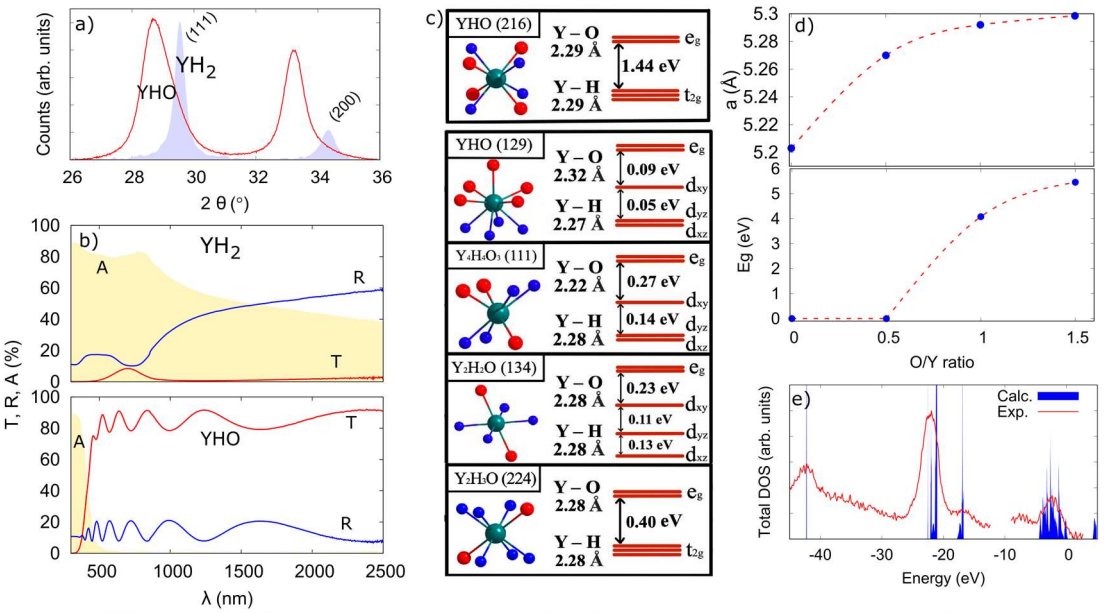

Figure 2.3 : XRD patters [panel (a)] and optical properties of transmittance T, reflectance R, and absorbance A [panel (b)] corresponding to YH_2 compared to photochromic yttrium oxyhydride (YHO). Schematic presentation of the bond coordination around Y, Y-O, and Y-H bond lengths, and splitting of the Y3d states at the conduction-band minimum for YHO of different stoichiometries, YH_xO_y, where yttrium, hydrogen, and oxygen atoms are presented as green, blue, and red spheres, respectively [panel (c)]. Calculated lattice constant and band gap [panel (d)] as a function of O/Y ratio in the YH_xO_y system. Total density of states from ab initio calculations as compared to experimental results from XPS measurements [panel (e)].

The oxygen intake also causes the band-gap opening. Figure 2.3(b) shows the experimental transmittance (T), reflectance (R), and absorbance (A) corresponding to YH_2 and compared to photochromic YHO. YH_2 presents the optical behavior of a metal, but after the incorporation of oxygen it turns into YHO, a wide-band-gap semiconductor. The role played by the ambient humidity has not been studied yet.

Taking the crystalline structure of YH_2 as the starting point [fm-3m and space group symmetry number (SPGN) 225], we build diverse YHO lattices of stoichiometry YH_2, Figure 2.3(c). In particular, multiscale modeling [57] predicted the possibility of lattices of stoichiometry (i) $Y_4H_4O_3$ 111 P$\bar{4}$2m and (ii) Y_2H_2O 134 P42/*nmm* [74], as well as (iii) YHO and SPGN 129 P4/*nmm*, 215 P$\bar{4}$3m, 224 P*n*$\bar{3}$*m*, and 216 P$\bar{4}$3*m*.

Systematic theoretical and experimental studies [3] pointed to P$\bar{4}$3*m* with SPGN 216 as the most energetically favorable yttrium oxyhydride lattice, i.e., stoichiometry x=1 and y=1 in YH_xO_y. In this structure, oxygen, as well as hydrogen atoms, are located in

tetrahedral sites. The x=1 and y=1 stoichiometry is consistent with the recent exhaustive compositional experiments [26,29].

YH_2 (225), $Y_4H_6O_2$ (224), Y_2H_2O (134), as well as $Y_4H_4O_3$ (111), present a metallic character, whereas YHO (216) is predicted to be a wide-band-gap semiconductor, as expected experimentally. According to these results, YHO crystallizes into a cubic structure with a lattice constant a = 5.29 Å, which corroborates the lattice expansion that takes place in YH_2 (a = 5.20 Å) when exposed to air. In particular, the expansion of a and the opening of the band gap after air exposure is predicted by DFT, see Figure 2.3(d). The calculated lattice constant and band gap are plotted as a function of the Y/O ratio. The predicted value of a for YHO is, however slightly smaller than the experimental value observed (a=5.34 Å) [1,3]. Discrepancies may arise from the difficulty in measuring a due to the lattice strains, defects, or other deviations from ideality in these thin films.

The Y, O, and H atoms occupy the Wyckoff positions 4c (1/4; 1/4; 1/4), 4a (0,0,0), and 4*b* (1/2, 1/2, 1/2), respectively, in this energetically favorable YHO (216) lattice. YHO belongs to the emerging family of materials called oxyhydrides [3]. The partial oxidation of YH_2 , and hence the formation of YHO, triggers the expansion of the unit-cell volume [74]. As a consequence of the lattice expansion, the bond distances in YHO will be subjected to oxygen-induced elongation, Figure 2.3(c). We show there the Y-O and Y-H bond lengths and the splitting of the Y3d states at the conduction band minimum for different YH_xO_y stoichiometries.

The experimental XPS data and the calculated total density of states of YHO (216) are in good agreement, as shown in Figure 2.3(c). The opening of a wide band gap as the oxygen atoms are incorporated in the YH_2 structure is also predicted by the ab initio calculations, Figure 2.3(d). However, the model overestimates the band gap. The calculated value of 4.9 eV for YHO (216) is about 1 eV larger than the experimental bandgap determined in the photochromic films by optical methods [3,14].

It should be noted that the YHO films, obtained by the oxidation of YH_2 previously prepared by reactive sputtering, are polycrystalline and multiphase in nature—note the widening of the XRD peaks of YHO when compared to YH_2 in Figure 2.3(a). Therefore, the energy-band diagram of the material most likely corresponds to a heterostructure of type II with a staggered band gap.

Assuming YHO (216) as the possible structure of photochromic yttrium oxyhydride, we can now explain the photochromic effect. The projected density of states (DOS) for YHO (216) revealed that both O and H atoms strongly contribute to the topmost valence band states. However, they are not hybridized because both H and O atoms are connected to the Y atoms independently from each other. On the other hand, the lowest conduction band is triply degenerate and formed mostly by Y d states, in particular, t_{2g} states, Figure 2.3(c). This result suggests that the light-induced O released from the film can be caused by the pseudo Jahn-Teller distortion effect: Y atoms are located at the center of the tetrahedral H and O sublattices. Under illumination, the transfer of electrons from the valence band to the t_{2g} bands will turn the YHO (216) lattice unstable [75].

As the p orbitals of O atoms are hybridized with the Y d orbitals, the degeneracy of the t_{2g} states can be avoided by the removal of oxygen atoms. As a result, an O-deficient unit cell with smaller lattice constant will be created. As reported by Pishtshev et al. [74], there are many O-deficient structural arrangements that can be obtained from YHO, Figure 2.3.

Before illumination, yttrium cations are in the oxidation state 3+, which is the very stable state. After illumination, some (very few [17]) of the O atoms will be detached from the Y^{3+} cations. Those Y atoms evolve from a 3+ to 2+ oxidation state, which is less stable. In darkness, the Y^{2+} atoms oxidize back to Y^{3+} by the incorporation of oxygen atoms that remained within the lattice [73], Figure 2.1(c), or newly incorporated from air.

As a result of illumination, metallic domains of smaller lattice constant will be created in the YHO (216) lattice, which results in the photochromic effect and the lattice contraction observed experimentally. The material seems to be able to host the out-diffused O atoms, which in some cases can reach the surface or even leave the film as demonstrated before. After stopping the illumination, the released O atoms can return to their former positions and the initial optical transparency will be restored.

2.4 Conclusions

When exposed to air the YH_2 lattice expands from 5.20 to 5.34 Å due to the incorporation of oxygen. In addition to the lattice expansion, YH_2 turns into YHO.

YHO is transparent and photochromic. The reversibility of the photochromic effect depends on the surroundings of the films, being a source of oxygen necessary for the adequate bleaching of the samples. Therefore, the photochromic mechanism must involve oxygen diffusion and oxygen exchange between the sample and its surroundings. A consequence of the oxygen diffusion is the unusual enhancement of the hydrophobicity and the reversible lattice contraction of the YHO films under illumination. Although further studies are needed, a preliminary theoretical study points to the pseudo Jahn-Teller effect as the possible cause of this light-induced oxygen diffusion observed YHO films.

2.5 Acknowledgements

This work has been supported by the Norwegian Research Council through the FRINATEK Project No. 287545, an internal project of the Institute for Energy Technology, and a Turkish Council of Higher Education Board 100/2000 Ph.D. scholarship. The computations were performed using the Norwegian Notur supercomputing facilities through Project No. nn4608k.

The authors contributed in the following ways—E.M.B: deposition of the YHO films, study of wettability, structural and optical properties of the YHO films; J.M.: deposition of the YHO films, study of structural and optical properties of the YHO films, cyclic optical measurements, XPS measurements, photochromic mechanism explanation, breathing concept, planning and formulation of conclusions; E.S.: DFT modeling of YHO. E.O.Z.: supervision on wettability measurements. S.K.: scientific supervision and support of the work, planning of experiments, mechanism of the effect, and formulation of conclusions; participation in DFT modeling. The paper was cowritten by J.M., E.M.B., and S.K. with the input of the rest of the authors.

3. PREFERENTIAL ORIENTATION OF PHOTOCHROMIC GADOLINIUM OXYHYDRIDE FILMS[2]

3.1 Introduction

Rare-earth metal oxyhydride (REMOH) thin films have attracted increasing interest during recent years due to their reversible photochromic properties at room temperature and ambient pressures [2,17,24,26]. Until now, the structure, chemistry and many properties of oxyhydrides have yet to be fully explored and almost no data is available in the usual material databases for rare-earth oxyhydrides [7]. Having multi-anion structures, rare-earth oxyhydrides present a high level of flexibility for material development thanks to the combination possibilities provided by two different anions: hydride and oxide. Besides powder production with a tube furnace [6,76], rare-earth metal oxyhydride films have also been successfully produced by reactive magnetron sputtering [3,24,28] and e-beam evaporation [4]. Typically, the synthesis consists of few steps. First, a di-hydride precursor film [3,26,28] is deposited onto a substrate (e.g., glass). It is then oxidized by exposure to air, resulting in photochromic polycrystalline oxyhydride films [73]. Several studies further attempted at each time to reveal the mechanisms of photochromism in rare-earth metal oxyhydrides through time resolved X-ray diffraction using synchrotron radiation [11], composition analysis [26,28,77] and positron annihilation spectroscopy (PAS) [78,79]. However, the answer for the exact mechanism for rare-earth metal oxyhydrides still debated.

The first study of gadolinium with varying levels of oxygen and hydrogen (GdO_yH_x) was carried out by Miniotas et al. [33], who reported gigantic resistivity, as well as band gap differences arising from compositional variations, i.e., a different hydrogen to oxygen ratio. However, the discovery of the photochromic properties of gadolinium oxyhydride (GdHO) had to wait until recently, when Nafezarefi et al. [24] reported

---

[2] This chapter is based on the paper: Baba, E. M., Montero, J., Moldarev, D., Moro, M. V., Wolff, M., Primetzhofer, D., Sartori, S., Zayim, E., Karazhanov, S. (2020). Preferential orientation of photochromic gadolinium oxyhydride films. *Molecules*, 25, 3181. https://doi.org/10.3390/molecules25143181 - Creative Commons Attribution 4.0 International license

GdHO films exhibiting photochromic contrast (differences in optical transmittance in dark and bleached state) around 45% after 8 h of illumination.

Generally, photochromic YHO thin films show a preferred growth along the [100] direction [11,80]. Phase diagrams and structural analysis have been reported for different REMOH (REM = Y, Sc or Gd) compounds, YHO being the most studied system. These studies claim that the fcc structure and phase diagram for YHO can be extrapolated for other rare-earth metal oxyhydrides [28]. However, the correlation between crystalline orientation and photochromic performance has not been investigated. Different crystal orientations might facilitate or hinder transport phenomena, as it did in a previous study [12] where oxygen transport into the material was demonstrated to play an important role for the evolution of photochromic properties of YHO.

In the present paper, we studied how the optical, compositional and structural properties of photochromic GdHO thin films are affected by subtle changes in preferential growth, which are controllable as a function of the deposition parameters.

3.2 Results

Figure 3.1(a) shows the grazing-incidence X-ray diffraction (GIXRD) patterns for photochromic GdHO deposited at different *p* values measured under ambient air. The intensity parameter δ achieved its lowest and highest value for samples deposited at 5.8 Pa (δ = 0.328) and 1.5 Pa (δ = 0.818), respectively. All films showed preferential growth along the [100] direction when compared to the standard diffraction peaks of GdH2 (Joint Committee of Powder Diffraction Standards JCPDS, card number 00-050-1107). This reference standard pattern, where δ = 0.2537, is depicted as vertical lines in Figure 3.1(a). The average grain sizes deduced using the diffraction peaks (111), (200), (220) and (311) are plotted in Figure 3.1(b) as function of P. The grain size decreased with the increasing pressure P: the dependence was weak at P and below 2 Pa, was much stronger at intermediate pressures, $2 < p < 5$ Pa and diminished as P exceeded 5 Pa. It is well established through the Thornton diagram [81–84] that sputter deposition at higher pressures results in the opening of inter-grain boundaries. Open inter-grain boundaries in the precursor gadolinium hydride films resulted in a higher surface area and faster oxidation kinetics. Consequently, the precursor hydride films deposited at higher pressures resulted in oxyhydrides with a higher oxygen content.

Time-of-flight energy elastic recoil detection analysis (ToF-E ERDA) (Figure 3.5) confirmed a higher oxygen content in samples deposited at higher *p*, which resulted in films with a wider band gap (Table 3.1). The band gap values of all samples are presented in Table 3.1. With increased deposition pressure, the band gap increased by 1 eV, approaching the value for Gd_2O_3. The presence of a Gd_2O_3 phase can explain the band gap widening (Table 3.1) and the reduced photochromic response (Figure 3.4) observed in samples obtained from precursor hydrides deposited at higher *p*.

Previous studies performed on YHO [18] suggested that variations of the band gap as a function of *p* were the result of changes in the O content in the films. Later, the oxygen incorporation result with the increased band gap by controlling deposition pressure was established [29] through compositional analysis performed on YHO samples deposited at 1 Pa and 6 Pa. It was shown that oxygen and hydrogen are anticorrelated.

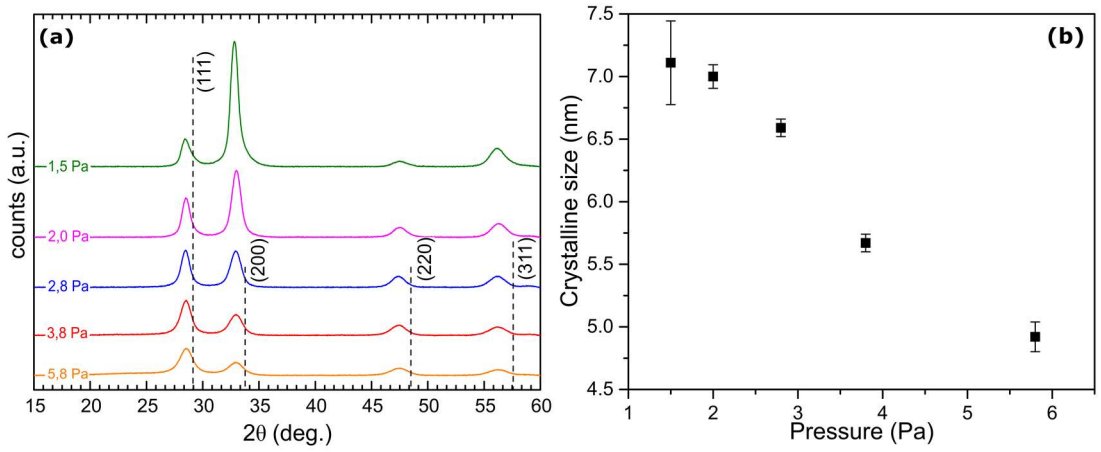

Figure 3.1 : Grazing -incidence X-ray diffraction (GIXRD) results for samples deposited at 1.5, 2.0, 2.8, 3.8 and 5.8 Pa. Photochromic films exhibited a change in the relative intensity of the different diffraction peaks as the oxygen incorporation increased due to the increase in deposition pressure. (b) The grain size reduced as a result of increased deposition pressure.

The compositional analysis performed in the present work also proved the anti-correlation between the O and H contents in the films. Figure 3.2(a) presents the O and H ratio as a function of p. Samples deposited at larger pressures were not included, as they presented low or no photochromism (Figure 3.4). The full depth profiles of oxygen and hydrogen can be found in the supplementary material, Figure 3.5. Figure 3.2 also displays the dependence of the photochromic contrast ΔT on *p*. Analysis

shows strong correlation between *p*, H content and ΔT, which is consistent with earlier findings [26] for YHO.

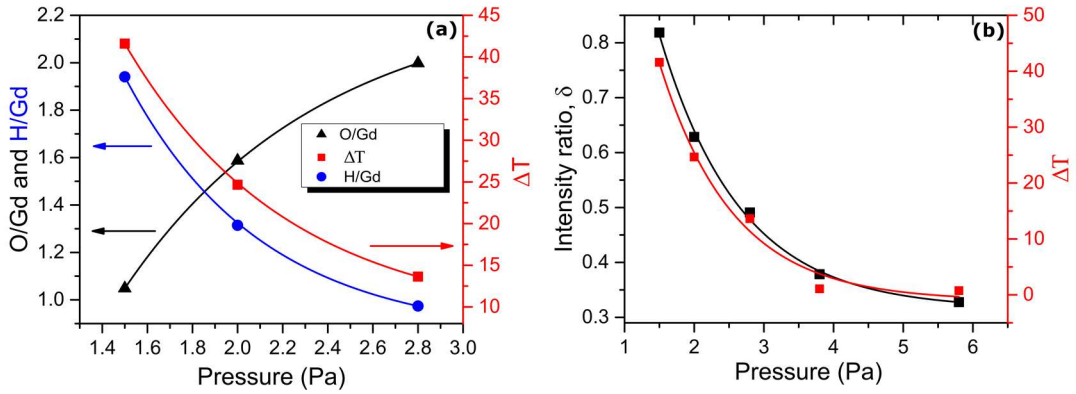

Figure 3.2 : (a) Composition of photochromic GdHO films and optical contrast ΔT as a function of deposition pressures. Optical contrast ΔT is averaged over wavelength 550 nm to 1000 nm. (b) Intensity ratio δ and ΔT as a function of deposition pressure. Curves are visual guides.

Figure 3.2(b) displays the dependence of δ and ΔT on *p*. By increasing *p* from 1.5 to 5.8 Pa, ΔT dropped from 40% to 0%, following the reduction of the intensity parameter δ. This decay with respect to deposition pressure clearly showed the strong correlation between preferential growth, optical properties, chemical composition and grain size of the GdHO films. The films with (200) orientation exhibit higher photochromic contrasts than the films with (111) orientation. It is well known for other oxides [85,86] as well as oxyhydrides [26] that changes in stoichiometry, specifically in oxygen content, result in changes in crystalline orientation and band gap. The experimental observations described above can be explained by a regulation of oxygen uptake through preferential orientation along the [100] direction.

It should be noted that the changes in the preferential growth can also be observed in yttrium oxyhydride (YHO) as a function of film thickness in films deposited under the same p [21]. However, preferential orientation was only reported at larger thicknesses (>~200 nm) with no indication of preferential growth in thinner films. According to our study, the lack of preferential growth along the [100] direction should result in smaller grain sizes and a low photochromic response when the film thickness is below 200 nm, in agreement with previous observations [21].

3.3 Materials and Methods

GdHO thin films with thicknesses ranging between 525 and 615 nm were reactively sputtered onto soda-lime glass substrates following a two-step deposition process [3,26,28]. First, gadolinium hydride (GdH_{2-x}) thin films were deposited by reactive pulsed DC magnetron sputtering from a metallic Gd target (purity 99.9%) in an H2/Ar atmosphere using a Leybold Optics A550V7 sputtering unit (Alzenau, Germany). The discharge power density was 1.33 W/cm_2 and the hydrogen-to-argon flow ratio (H_2/Ar) was kept at 0.22. The deposition pressure p was varied from 1.5 to 5.8 Pa by adjusting a throttle valve placed between the deposition chamber and the vacuum line. The deposition process was carried out without an intentional heating of the substrate. In a second step, the GdH_{2-x} films were oxidized when they were removed from the chamber and were exposed to air, thus turning into a transparent and photochromic GdHO.

The thickness of the films was measured using a Step-200 profilometer (Milpitas, CA, USA). The crystallographic structures of the films were characterized by grazing-incidence x-ray diffraction (GIXRD) in a Bruker Siemens D5000 (CuKα radiation, parallel beam geometry and 2° angle of incidence, (Billerica, MA, USA). Grain sizes were calculated using the Scherrer equation [87], assuming spherical crystals;

$$L = K\lambda/\beta \cos\theta, \tag{3.1}$$

where L is the grain size, K is the shape factor chosen as 0.9, λ is the wavelength, β is the peak broadening at half maximum and θ is the diffraction angle.

Further, we defined the intensity ratio parameter δ [85] as:

$$\delta = I_{(200)}/[I_{(111)} + I_{(200)}], \tag{3.2}$$

where $I_{(111)}$ and $I_{(200)}$ are the intensities of the [111] and [100] diffraction maxima.

Optical transmittance T, reflectance R and absorptance A of the GdHO films in the clear and photo-darkened state were obtained with an integrated sphere using an Ocean Optics QE6500 spectrophotometer (Dunedin, FL, USA). The photochromic contrast was defined as $\Delta T = T_{clear} - T_{dark}$, where T_{clear} and T_{dark} were the transmittance in the clear and photo-darkened state, respectively. Analogously, the photochromic contrast in A and R were defined as $\Delta A = A_{clear} - A_{dark}$ and $\Delta R = R_{clear} - R_{dark}$.

The photochromic effect was triggered by a 6 W-lamp (wavelength 405 nm). Cyclic illumination was performed using a 405 nm-laser (4.5 mW). The absorption coefficient α was calculated from T and R values;

$$\alpha = d^{-1} \ln((1 - R^2)/T), \quad (3.3)$$

where d is the film thickness. The absorption coefficient is related to the energy Eg of the optical band gap [88]:

$$\alpha h\nu^m = \alpha_0(h\nu - E_g), \quad (3.4)$$

where hν is the energy of incident photon, α_0 is a constant and m is a factor that depends on the optical transition (m = 2 for direct-allowed and 1/2 for indirect-allowed transitions) [89].

Chemical composition analysis was performed by coincidence time-of-flight energy elastic recoil detection analysis (ToF-E ERDA) at the Tandem Laboratory of Uppsala University. In this work, projectiles of 36 MeV 127I8+ were used as a probe beam and the recoiled specimens were detected by a telescope ToF-E tube placed at 45° with respect to the beam's direction [90]. A detailed discussion about the ToF-E ERDA setup used on similar samples (YHO) can be found elsewhere [77].

3.4 Conclusions

We studied GdHO films deposited onto glass substrates in an H_2/Ar plasma prepared at different sputtering pressures. The influence of deposition parameters and film composition on the photochromic performance was systematically studied. We demonstrated that the preferential growth of GdHO films can be controlled by the variation of the deposition pressure. Highly oriented (200) films were formed at deposition pressures ≥1.5 Pa. The photochromic contrast >20% was found for films deposited at ≤2.8 Pa. Within this study, we also established band gap control from 2.8 eV to 3.7 eV over reactively sputtered gadolinium oxyhydride films. We revealed an inverse correlation between deposition pressure and photochromic contrast in GdHO, determined by the oxygen content. Higher deposition pressures during the fabrication of the hydrides resulted in a higher degree of oxygen incorporation, followed by the reduced photochromic response when the sample was exposed to air, forming the

oxyhydride. We also showed that increasing oxygen incorporation is related to the preferential orientation changes of the lattice from [100] towards the [111] direction.

3.5 Supplementary Materials

3.5.1 Optical characterization

Figure 3.3 shows (a) optical transmittance T and (b) absorptance A as a function of wavelength λ and photon energy E, respectively, for photochromic GdHO samples (clear state) deposited at pressures P ranging from 1.5 to 5.8 Pa. As P increases, T increases in the visible regime between 400 and 700 nm (a) and the absorption edge, located at shorter wavelengths, shifts towards higher energies (b).

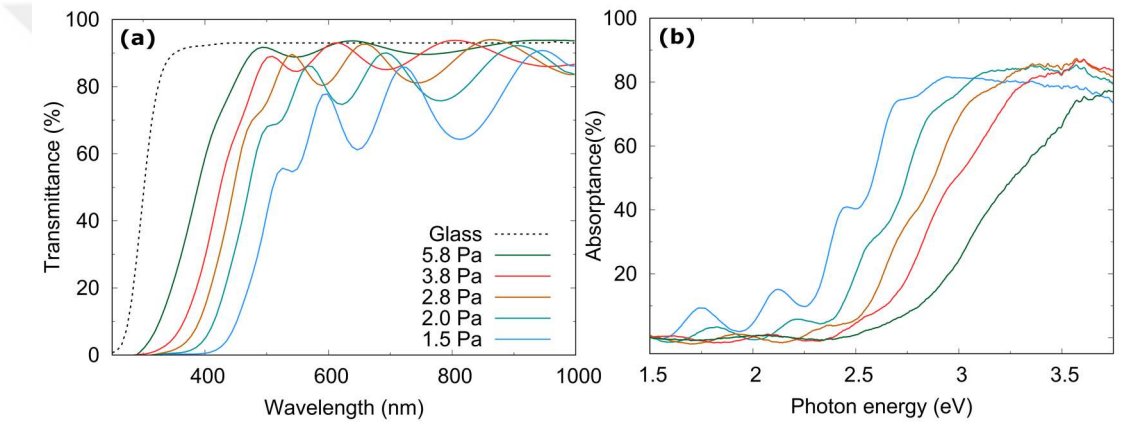

Figure 3.3 : Transmittance (a) and absorptance (b) of photochromic gadolinium oxyhydride films reactively sputtered at deposition pressures between 1.5 and 5.8 Pa.

Figure 3.4 shows the difference in (a) transmittance ΔT, (b) absorptance ΔA and (c) reflectance ΔR for films deposited at different P before and after illumination. The absorption edge shifts towards shorter wavelengths with increasing P indicating a widening of the bandgap (bandgap energies are tabulated in Table 3.1). E_g^{dir} increases from 2.8 to 3.7 eV as P increases from 1.5 to 5.8 Pa.

Figure 3.4(d) shows the absorptance averaged between 550 nm and 1000 nm in the clear A_{clear} and photodarkenened A_{dark} states, as well as the photochromic response $|\Delta A|$ as a function of deposition pressure. The photochromic response decreases as P increases (e.g., P = 1.5 Pa, $|\Delta A|$ = 47 % and P = 5.8 Pa, $|\Delta A| \approx 0$ %). These results, which are consistent with previous reports [18], are attributed to the increase of oxygen content in the films prepared at larger P, resulting in higher porosity [91], favoring

thus the exchange of hydrogen and oxygen once the samples are removed from the sputtering chamber and exposed to ambient conditions [29].

Table 3.1 : Bandgap values of samples deposited between 1.5 Pa and 5.8 pa.; where E_g^{dir} refers to the energy of the direct bandgap.

Sample	Deposition pressure (Pa)	Film Thickness (nm)	E_g^{dir} (eV)
GdH_3			2.4[33]
GdHO	1.5	616	2.8
	2.0	575	3.0
	2.8	550	3.1
	3.8	525	3.3
	5.8	540	3.7
Gd_2O_3			5.4[92]

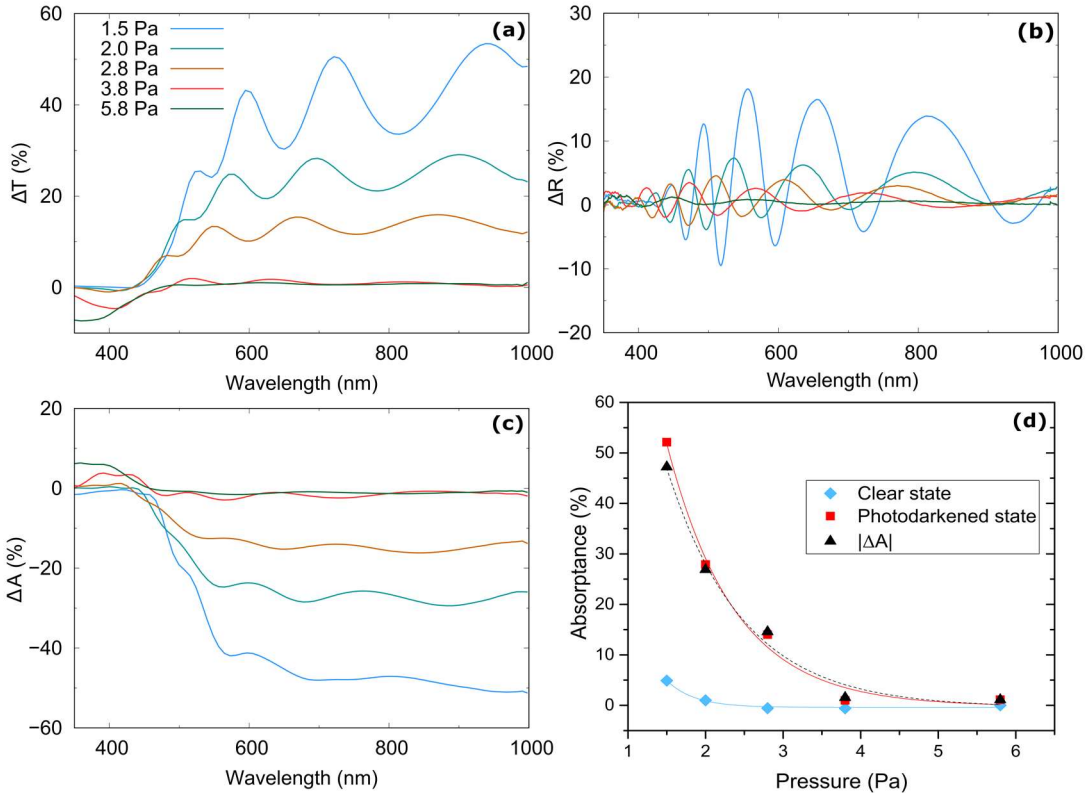

Figure 3.4 : Change in (a) transmittance, (b) reflectance and (c) absorptance of samples plotted versus wavelength, deposited between 1.5 Pa and 5.8 Pa before and after 60 minutes of illumination. (d) Absorptance and photochromic response, averaged between 550-1000 nm, of samples plotted versus pressure.

3.5.2 Compositional analysis

Figure 3.5(a and b) shows normalized and interpolated maps of the O and H content as a function of deposition pressure and depth. C impurities of up to 4 at. % are not indicated. All the majority elements (i.e., Gd, O and H) are uniformly distributed throughout the films, except at the surface, where an oxygen-rich layer (within 5-10 nm) is found. The increase in deposition pressure leads to stronger oxidation and decrease of hydrogen content. This effect can be attributed to variations of the porosity of the films [91]. The replacement of H atoms by O atoms during the oxidation process is suggested by the anti-correlation in the O and H content (Figure 3.5). Typical uncertainties - statistical and systematic - involved in this measurement, especially towards lighter elements as H, are discussed in detail using similar system elsewhere [77].

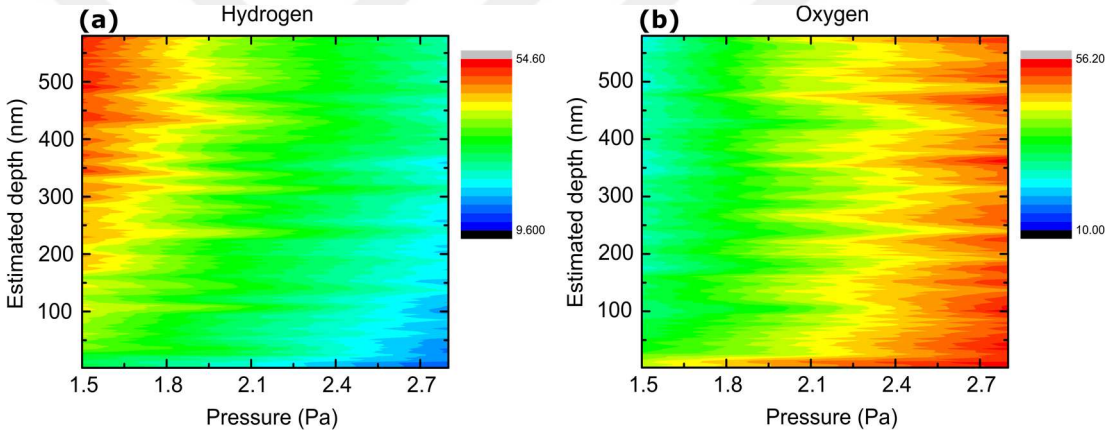

Figure 3.5 : Depth profiles of (a) hydrogen and (b) oxygen plotted versus deposition pressure deduced from Tof-E ERDA coincidence spectra (not shown).

3.6 Author Contributions

Conceptualization, E.M.B., J.M. and S.K.; methodology, E.M.B. and J.M.; formal analysis, E.M.B., J.M., D.M., M.V.M., M.W., D.P., S.S., E.Z., S.K.; investigation, E.M.B., J.M., D.M., M.V.M., S.K.; resources, S.K.; data curation, E.M.B., D.M., M.V.M.; writing—original draft preparation, E.M.B.; writing—review and editing, E.M.B., J.M., D.M., M.V.M., M.W., D.P., S.S., E.Z., S.K.; visualization, E.M.B., D.M., M.V.M.; supervision, E.Z., S.K.; project administration, S.K.; funding acquisition, S.K. (FRINATEK Project No. 287545 from the Research Council of Norway), D.P. (infrastructural grants from VR-RFI and SSF). All authors have read and agreed to the published version of the manuscript.

3.7 Funding

The work by IFE team has received funding from the Research Council of Norway through FRINATEK Project No. 287545. Accelerator operation at Uppsala University is supported by the Swedish Research Council VR-RFI (contract No. 2017-00646_9) and the Swedish Foundation for Strategic Research (contract RIF14-0053).

4. TEMPERATURE-DEPENDENT PHOTOCHROMIC PERFORMANCE OF YTTRIUM OXYHYDRIDE THIN FILMS[3]

4.1 Introduction

Photochromism is the phenomenon in which the optical properties of a material are altered due to the absorption of electromagnetic radiation. This effect can be utilized for a broad range of applications, with a specific focus on smart windows, displays, and energy-saving applications. While it is well known that yttrium hydride (YH_x) [9] exhibits photochromic properties at high pressures (GPa), it was recently demonstrated that rare earth metal oxyhydrides exhibit similar photochromic behaviors at ambient conditions [2,24]. The remarkable advantage of the latter class of materials is the ability to deposit thin films at room temperature using, e.g., magnetron sputtering [3,24,28] or electron-beam evaporation [4], with little to no additional processing, which offers excellent scaling potential for industrial applications. It was recently shown that rare-earth oxyhydrides can also be synthesized as bulk samples [5]. Furthermore, the ability to incorporate different anions offers tantalizing possibilities for creating new materials with unique properties that are not possible with single-anion compounds [7]. However, many of the fundamental properties of rare-earth metal oxyhydrides have yet to be understood, which has hindered their widespread use in applications.

Of the rare-earth metal oxyhydrides, yttrium oxyhydride (YHO) has been a strong subject of recent experimental [2,8,11,21,79] and theoretical [30,93] investigations. Thin films of YHO exhibit photochromic behavior, in which a decrease in the transmittance, and consequently an enhancement of light absorption, of the films (referred to as photodarkening) is observed upon illumination with photons with energies between 1.8 and 3.1 eV [8,18]. The photodarkening rate has been shown to

[3] This chapter is based on the paper: Baba, E. M., Weiser, P. M., Zayim, E. Ö., Karazhanov, S. (2020). Temperature-dependent photochromic performance of yttrium oxyhydride thin films. *Physical Status Solidi RRL*, 2000459 (1 of 5). https://doi.org/10.1002/pssr.202000459 - Creative Commons Attribution 4.0 International license

depend on both the intensity and the energy of the illuminating light. Removal of the illumination is followed by recovery of the film's transmittance to the initial, transparent state (referred to as bleaching). Yttrium atoms in photochromic YHO have been shown to possess mixed oxidation states, either +2 or +3 [26]. Initially, the darkening process was postulated to arise from the formation of dilute metallic domains that arise from photo-induced changes in the charge state of Y [14,17]. Recently, oxygen was shown to play a key role in the photochromic process of YHO [12]. Indeed, photodarkened YHO thin films bleach back to their transparent pre-illuminated state much more rapidly in air than in an inert ambient. It was proposed that the photochromic process could be explained in terms of light-induced breathing, whereby the exchange of oxygen atoms between the films and the ambient atmosphere during the darkening and bleaching processes results in contraction and expansion of the YHO lattice, respectively. Despite these observations, the fundamental mechanism for anion diffusion and its connection to the photochromic behavior of YHO is not well understood.

In this work, we use transmittance infrared (IR) spectroscopy to study the dependence of photodarkening and bleaching of photochromic YHO thin films on temperatures in the range of 5 and 295 K. The photodarkening process of photochromic YHO demonstrates no dependence on temperature, as YHO can photodarken after exposure to UV light at temperatures as low as 5 K, where anion diffusion is expected to be highly limited. Bleaching of the films, however, is strongly influenced by temperature: a small recovery of the transmittance is observed between 5 and 50 K, whereas a slow, stepwise recovery occurs between 100 and 250 K. Based on our results, we suggest that anion diffusion does not contribute to the darkening or bleaching processes at low temperatures, and that other mechanisms, e.g., charge transfer, are needed to fully explain the photochromic process.

4.2 Experimental Details

Thin films of metallic yttrium hydride (YH_{2-x}) were deposited onto glass substrates using reactive magnetron sputtering under deposition pressures (P_d) of either 1 or 1.5 Pa. Post-deposition oxidation to convert YH_{2-x} to YHO was performed by exposing the films to ambient air at room temperature in accordance with the processing conditions reported in the literature [3,14] The photochromic behavior of the films

implies that the H:O ratio falls within the range determined from compositional analysis measurements [26,28]. The films were subsequently stored in an inert atmosphere (N_2). The thicknesses of the synthesized YHO films, as measured using a Step-200 profilometer, were found to be 1250±50 nm.

Infrared (IR) transmittance spectra were measured using a Bruker IFS 125HR Fourier Transform spectrometer purged with dry N_2 gas and equipped with a quartz light source, a CaF_2 beam splitter, and a liquid-nitrogen-cooled InSb detector. All measurements utilized a spectral resolution of 4 cm^{-1} with the empty sample holder serving as the background single-channel spectrum. The samples were cooled in He exchange gas in a Janis PTSHI-950-5 low vibration pulse tube cryostat equipped with two sets of ZnSe windows. The temperatures of the samples were varied between 5 and 295 K (±1%) using a Lakeshore Model 335 temperature controller. The sample holder was rotated such that the unpolarized IR beam was incident at an angle of 40±3° on the surface of the film. Photodarkening experiments were performed by illuminating the films with a collimated UV laser diode (ThorLabs CPS405, λ=405±5 nm, 4.5 mW power) along the direction perpendicular to the IR beam path and through two sets of sapphire windows. This geometry allowed variable temperature measurements of the optical transmittance during UV illumination. The IR beam aperture was set to 0.5 mm and focused within the UV-illuminated part of the film. Bleaching experiments were performed using the same geometry as the darkening ones but with the UV laser diode blocked. The photochromic performance was evaluated using the difference in the transmittance $\Delta T(\nu, t) = T_i(\nu, 0) - T_f(\nu, t)$ between initial (*i*) and final (*f*) states. Here, T is transmittance, ν is wavenumber (cm^{-1}), and t is the time between states *i* and *f*. For our analysis, we consider the value of ΔT averaged between 4000 and 12000 cm^{-1}.

4.3 Results and Discussion

Figure 4.1 shows the evolution of the IR transmittance spectra at 295 K of YHO thin films deposited with P_d =1.0 and 1.5 Pa during photodarkening under UV light (panels (a) and (c), respectively), and during bleaching when the UV light is removed (panels (b) and (d), respectively).

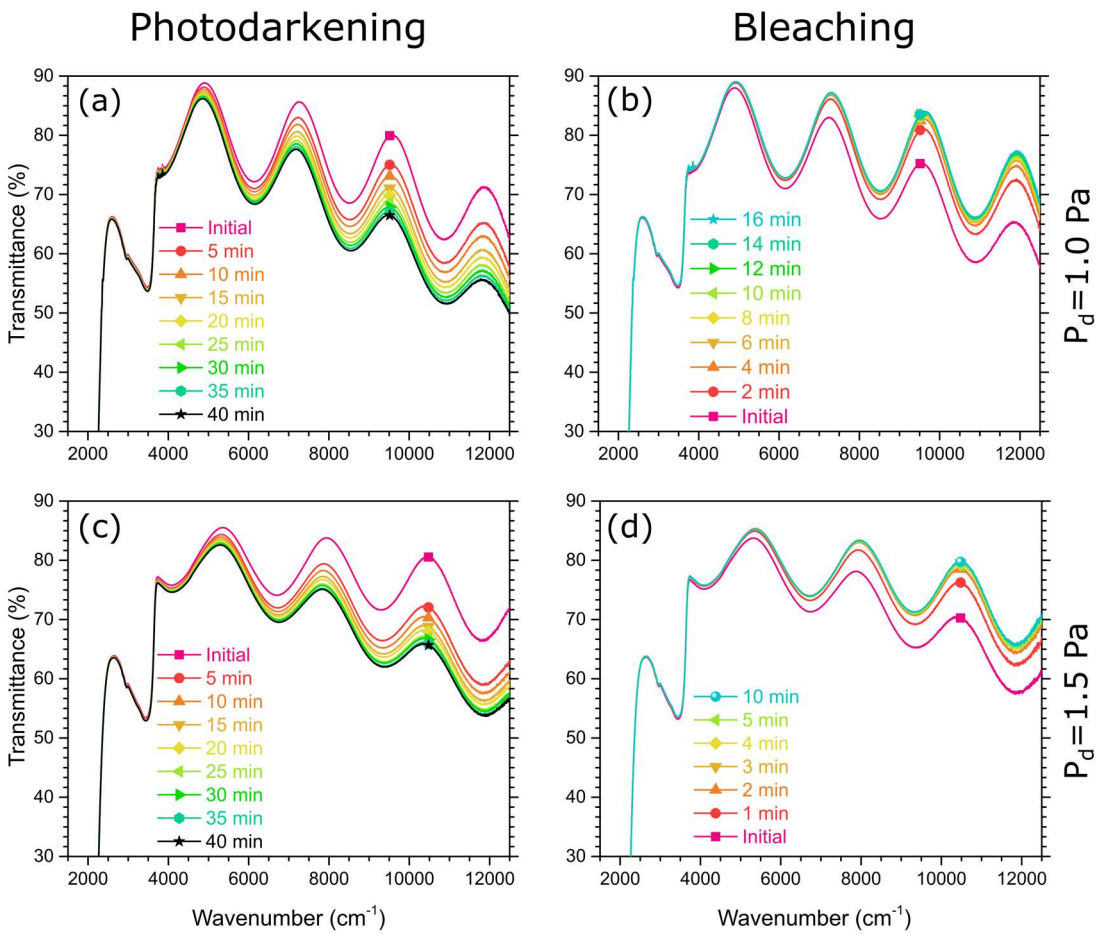

Figure 4.1 : Infrared transmittance spectra (solid curves) of photochromic YHO thin films at 295 K during photodarkening for between 0 and 40 minutes [(a) and (c)] and during subsequent bleaching for between 0 and 16 minutes [(b) and (d)]. The upper [(a) and (c)] and lower [(b) and (d)] panels are for the films deposited at 1.0 and 1.5 Pa, respectively.

For both films, ΔT increases with increasing energy of the incident light, which is in accordance with previous reports in the literature [2,3,14,24]. After 40 minutes of UV illumination, the photodarkened films show an average ΔT over the range from 4000 and 12000 cm^{-1} of about 8%. Upon removal of the UV illumination, the YHO thin films begin to bleach, and the initial transparencies of the films are recovered within 16 min (P_d =1.0 Pa) and 10 min (P_d =1.5 Pa).

Following this recovery, the films were cooled (without UV illumination) to 5 K and subsequently UV illuminated to produce the photodarkened state. Panels (a) and (b) of Figure 4.2 show the evolution of the IR transmittance spectra measured at 5 K during the photodarkening process for the two YHO films shown in Figure 4.1. (The increase in temperature of the films due to UV illumination is not more than 1-2 K.) The corresponding ΔT for the films are shown in Figure 4.2 (c) and (d). Compared to the

process at 295 K, photodarkening of the films at 5 K results in higher photochromic contrast (ΔT=~26% and 14% for P_d=1.0 and 1.5 Pa, respectively) and faster initial darkening rate. We caution, however, that the photochromic response in YHO thin films is known to be affected by other factors, e.g., deposition pressure [18] and previous darkening-bleaching cycles (so-called memory effect) [2]. The deposition pressure is inversely related to the photochromic contrast and, has been demonstrated for both YHO [18,29] and a related material, gadolinium oxyhydride [31]. The memory effect caused by consecutive darkening-bleaching cycles leads to higher photochromic contrast and faster photodarkening rates, which is consistent with the photodarkening behavior observed at 5 K.

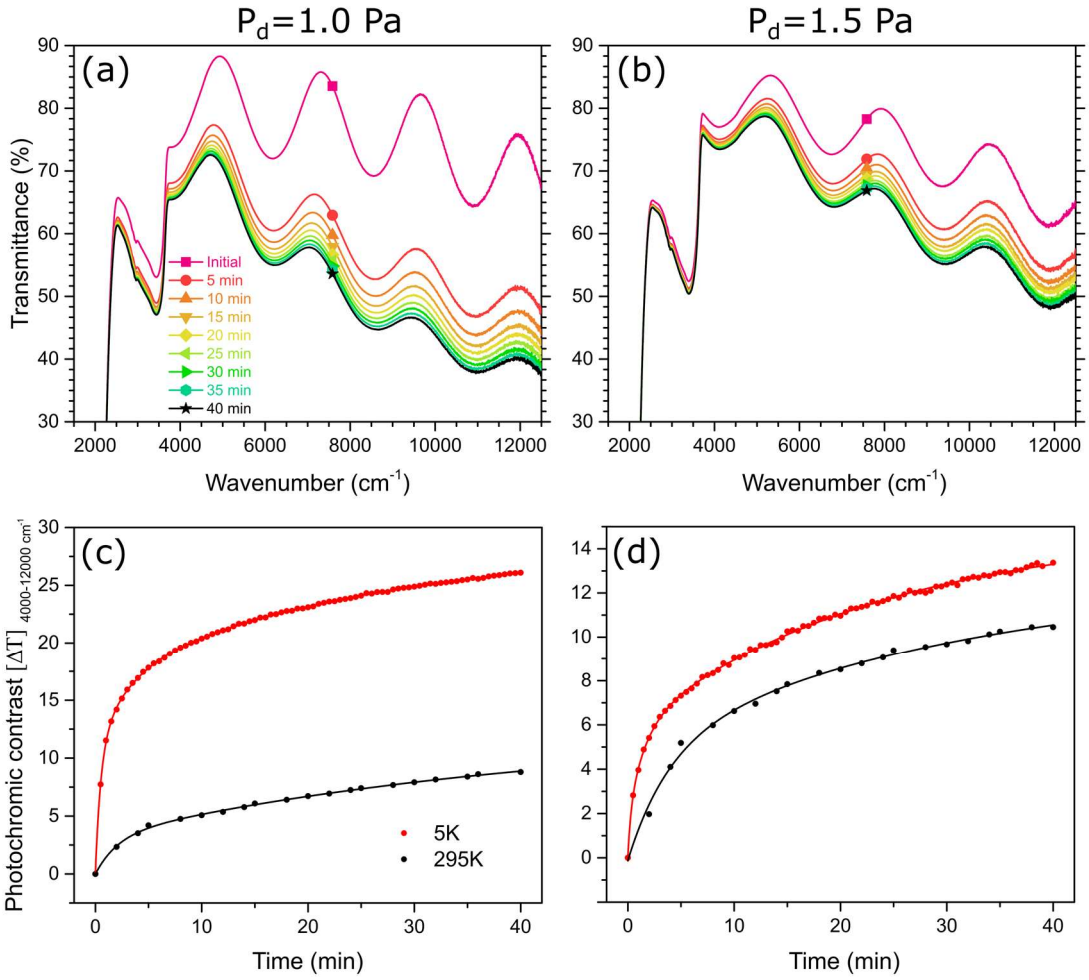

Figure 4.2 : Infrared transmittance spectra (solid curves) of photochromic YHO thin films in their initial transparent state and after photodarkening at 5 K between 5 and 40 minutes for samples deposited at (a) 1 Pa and (b) 1.5 Pa. The average photochromic contrast (filled circular points) as a function of the UV illumination time is shown in panels (c) and (d) for the films deposited at 1.0 and 1.5 Pa, respectively. Here, the solid lines serve as guides to the eye.

Additional experiments are needed to fully elucidate the individual effects of photodarkening temperature and deposition pressure from those due to memory on the photochromic performance. It should also be noted that the photochromic contrast in the IR spectral region where O-H vibrations typically occur (3000-3500 cm^{-1}) exhibits a significant ΔT at 5 K compared to the essentially null change at 295 K. Such a change might be indicative of the presence of and changes to OH-related species, but our data do not allow us to draw a definitive conclusion at this time.

The mechanism(s) responsible for the photochromic effect observed in YHO, as well as other rare-earth metal oxyhydride, thin films is still under debate. In YHO thin films, it was recently suggested that oxygen out-diffusion from the lattice followed by formation of metallic YHO domains is necessary for the photodarkening process [12,17]. In contrast, it was proposed that photon-induced hydrogen transfer between phases [13,37] could also explain the photochromic mechanism. In either case, the ability of the films to achieve the darkened state at 5 K suggests that anion transfer is not responsible for this process at low temperatures. Furthermore, if the photodarkening process relied solely on anion transport, then a lower illumination temperature should decrease the darkening rate, even accounting for memory effects. Instead, we observe that the darkening rate increases strongly at 5 K compared to 295 K. We propose, therefore, that the darkening process does not require in- or out-diffusion of anions from the film. Instead, we favor a model where charge transfer, by UV illumination-induced bond breakage, is responsible for photodarkening.

Given the extraordinary ability of the YHO thin films to photodarken even at 5 K, we have also investigated its effect on the bleaching process. Figure 4.3 shows the change in the average ΔT between 4000 and 12000 cm^{-1} vs. the time after the UV illumination was stopped (i.e., only the probing IR beam was incident on the sample) of the YHO thin films deposited at P_d=1.0 Pa (a) and 1.5 Pa (b) for temperatures ranging between 5 K and 250 K. These bleaching measurements started with the samples held at 5 K for a period of about 40 minutes, with a new spectrum acquired every 30 seconds. As can be seen in Figure 4.3, the film remains in its darkened state at 5 K, with only a small amount of bleaching ($\Delta T \approx 1.5$-2%) occurring even 40 minutes after the UV illumination was stopped. The average ΔT due to the drift of the spectrometer response over the same duration is <0.7%. Furthermore, transmittance measurements (not shown) of the YHO film deposited at P_d=1.5 Pa from 295 K to 5 K show that the films

remain transparent (ΔT<0.2%) while illuminated with the IR beam, i.e., the probing IR beam does not photodarken the films. Therefore, the small bleaching observed at 5 K is considered a real result and not an experimental artifact. Subsequent heating of the samples between 10 K and 50 K produced no significant change in ΔT. For temperatures between 50 K and 200 K, the samples were heated in steps of 25 K, with the set temperature stabilized to within ±0.5 K. Transmittance spectra of the films were measured until the bleaching rate slowed considerably, which was typically after 5-10 minutes. Above 200 K, the samples were heated in temperature steps of ~50 K (with the set temperature stabilized to within ±0.5 K) for 10-15 minutes until the transparent state was fully recovered. In both cases, transmittance spectra were acquired every 30 seconds. Bleaching of the films remained slow during heating for temperatures up to and including 100 K. Above 100 K, the bleaching process becomes stronger, with similar amounts (ΔT =4-5%) of transparency recovered at each temperature. These results establish that the bleaching of photochromic YHO thin films is a thermally driven process.

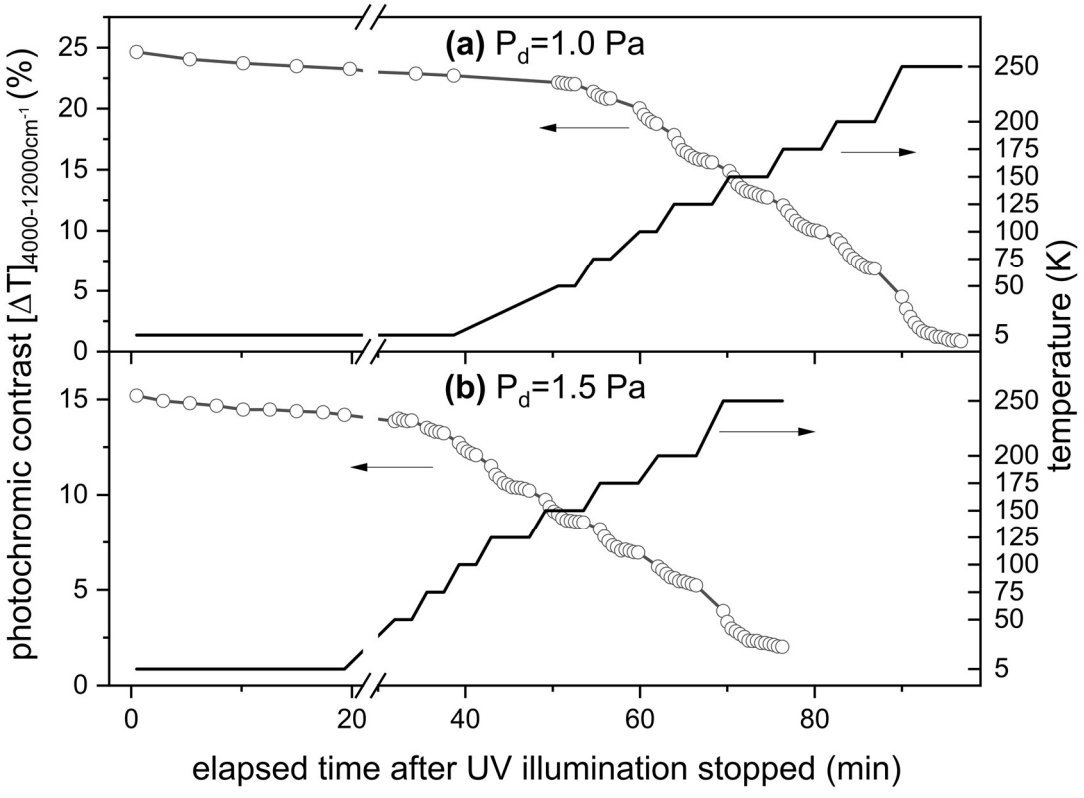

Figure 4.3 : Change in the photochromic contrast (open circles, left axis) of the photodarkened YHO thin films vs. the elapsed time after removal of the UV illumination, i.e., during the bleaching process. The temperature of the thin film during the measurement (solid curve, right axis) is indicated. The upper (a) and lower (b) panels are for the films deposited at 1.0 and 1.5 Pa, respectively.

The ability of the YHO films to recovery transparency below 100 K is remarkable because anion diffusion is considerably slowed down in this temperature range [94]. The prefactor and the thermal activation energy for hydride diffusion in YH_x (for x between 1.91 to 2.03) were shown to vary between (1.0-4.8)×10^{-4} cm^2 s^{-1} and 0.38-0.53 eV, respectively[94]. Assuming that the H^- diffusion parameters in YHO are similar to the ones for H^- in YH_x, then the diffusivity of H^- at 100 K is estimated to be ~10^{-30} cm^2 s^{-1}. The ionic radius of O^{2-} is similar to that of H^- [7,95], and, to first approximation, one could expect that the diffusion of O^{2-} will be similar or slower compared to that of H^-. Our results below 100 K indicate that anion transport should not solely be responsible for bleaching and that an additional mechanism (or mechanisms) is needed. We consider one possible mechanism that can explain the partial bleaching at low temperatures, which could potentially be the underlying mechanism for photochromism in rare-earth metal oxyhydrides: photo-driven charge transfer. Photochromic YHO consists of semiconducting and metallic phases when exposed to UV light [17], and interfacial charge transfer between these inhomogeneous domains could also explain the small recovery. Such a mechanism was recently proposed to explain the photochromic effect in MoO_3:TiO_2 crystalline-core amorphous-shell nanorods [96]. However, further studies on multi-phase systems and charge transfer in YHO are needed to fully understand the photochromic mechanism.

4.4 Summary

In summary, we have used IR spectroscopy to show that the photochromic performance of YHO thin films is dramatically influenced by temperature, which yields new insights into the fundamental mechanisms responsible for the photodarkening and bleaching processes. Both the ability of the films to photodarken at 5 K and the small amount of bleaching (ΔT~1.5-2%) that occurs between 5 and 50 K indicates that the photochromic behavior of YHO is not due solely to anion diffusion, either into or out of the film, as was previously postulated based on measurements at 295 K. The stepwise recovery of the transmittance at successively higher temperatures indicates that the mechanism(s) responsible for bleaching are complex and require further investigations to clarify their origin.

The temperature dependence of the photochromic behavior presents intriguing possibilities for YHO films that require materials and devices exhibit tunable optical

properties when subjected to extreme thermal changes in space, e.g., IR stealth [97,98], particularly between the in-sun and in-eclipse conditions. Given their common photochromic behavior, the conclusions regarding the darkening and bleaching processes could extend beyond YHO and into other rare-earth metal oxyhydride materials.

4.5 Author Contributions

All authors contributed equally to this work.

4.6 Acknowledgements

Funding for this work was provided by the Research Council of Norway through the FRINATEK project (#287545) the Norwegian Micro- and Nano- Fabrication Facility (NorFab, #245963), and the Center for Sustainable Solar Cell Technology (FME SuSolTech, #257639). We are grateful to E. Monakhov for his helpful discussions about the results and for proofreading the manuscript.

5. HUMIDITY INDUCED DEGRADATION OF PHOTOCHROMIC PROPERTIES OF YTTRIUM OXYHDRIDES

Yttrium oxyhydride (YHO) exhibits photochromic properties at room temperature. Although transparency in clear state, contrast and kinetics of color change present interest for applications, i.e., smart windows, durability of the films is limited because of delamination. After several cycles of illumination with UV light on and off or just storage in humid atmosphere, contrast of the films lost, and delamination starts. In this section, we report about mechanism of delamination of the YHO films by systematic study of the films in environment with different humidity.

Yttrium oxyhydride (YHO) present interest for applications in windows for reducing glare because of high transmittance in clear state (> 80%), contrast (>20%), fast coloration and bleaching times [3,14,18,21]. In order to realize YHO coatings into smart-window applications, environmental durability needs to be investigated. One of the limiting factors agains commercialization of YHO-based photochromic coatings in windows is delamination of the films from substrate that can happen after several cycles of illumination on/off with UV light or storage in humid atmosphere. Through systematic study it was shown that the reason of delamination is the interaction of the YHO films with humidity.

5.1 Methods

Oxygen free yttrium hydride (YHx) layers were deposited reactively in an atmosphere containing Ar (6N) and H_2 (6N) with H_2:Ar ratio of 0.21 at 1 Pa. Pulsed DC magnetron sputtering was performed by Leybold Optics A550V7 sputter unit and, followed by post-deposition oxidation in air to synthesize yttrium oxyhydride (YHO). Resulting layer thickness measured as 700±10 nm. Illumination studies were performed using Thorlabs narrow wavelength UV lamp with intensity peak at 405nm with 30 minutes illumination and 30 minutes storage under darkness. Thickness measurement were performed using Step-200 profilometer. Surface images were obtained using a Hitachi

S-4800 scanning electron microscope (SEM) with an acceleration voltage of 10 kV was used.

Humidity tests were performed using airtight boxes filled with saturated aqueous solutions [99] and molecular sieves where samples were placed right above the solutions, right after deposition. Relative humidity (RH) levels at 25ºC were up to 100% RH where RH levels (±1%) were set by using saturated aqueous solutions of Magnesium Chloride (Sigma Aldrich, 98%), Magnesium Nitrate (Sigma Aldrich, 99%) and Sodium Chloride (Sigma Aldrich, 99.5%) for 33%, 53% and 75% RH, respectively. The driest environment was prepared by 3Å molecular sieve filled desiccator, 100% RH by DI water. Also, samples stored for six months in a glovebox containing dry air (H2O < 0.9 ppm) for long term testing. Illumination studies were performed after samples stored for 2, 4 and 14 days.

5.2 Results

Figure 5.1 demonstrates the effect of water content in air on YHO photochromic performance over the duration of (a) 2 days and (b) 14 days. Photochromic as prepared YHO sample, first, characterized by 30 minutes UV illumination followed by 30 minutes in darkness. Sample demonstrated ≈25% contrast where transmittance averaged between 650-800nm. After samples were stored in desiccators with 33% RH, 53%RH, 75% RH, and 100%RH at 25ºC. For comparison with a dry environment effect, one sample placed in a desiccator filled with 3Å molecular sieves and another in a dry air glovebox for long term testing. After 2 days of storage (Figure 5.1 (a)), the sample stored in desiccator with 3Å molecular sieve shows almost no change in contrast where samples stored in desiccators with 53% RH, 75% RH and 100% RH environments show considerable loss as well as slight increase of clear state transmittance (T_{clear}) before UV illumination. Also, the sample stored in 33% RH environment lost small contrast (≈5%) but not as high as the sample stored in higher RH environments (>7%), indicating a slight trend. After 14 days of storage (Figure 5.1 (b)), all samples show contrast loss where a small change is shown by the sample stored in dessicator with 3Å moleculer sieve. Considering the desiccator filled with molecular sieves presents substantially low water content and still shows contrast loss, might indicate the degradation effect of even the residual water in the environment. Contrast loss of sample stored in desiccator with 3Å molecular sieve followed by the

sample stored in second lowest RH level of 33% (>7%). On the other hand, samples stored in 53%, 75% and 100% show similar (<8%) contrast losses after 14 days.

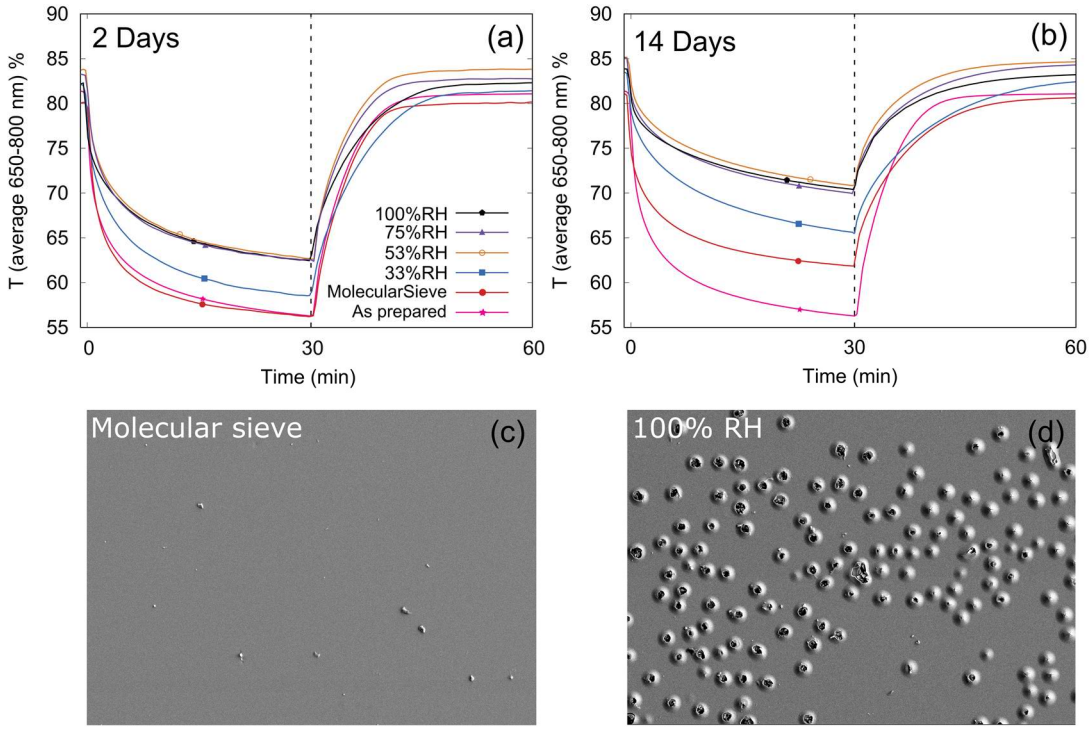

Figure 5.1 : Photochromic performance of YHO samples by 30 minutes UV illumination/darkness cycle were measured. Transmittance (averaged between 650-800nm) of samples after storing 3Å molecular sieve filled box, 33%, 53%, 75% and 100% RH at 25°C for (a) 2 days and (b) 14 days as well as SEM images for samples stored for 14 days in (c) dessicator (3Å molecular sieve) and (d) 100% RH at 25°C.

These results show that, YHO loses photochromic contrast with a substantial amount when stored in an environment with water presence higher than the water in air with 33% RH at 25 °C. Rate change for darkening and recovery might be a direct result of structural damage by the water which is known to dissolve rare-earth oxides [66]. To investigate the structural effect of water on YHO samples stored in varying RH levels, SEM images were taken after 14 days storage at respective environments and can be observed in Figure 5.1 (c-d). The sample stored in desiccator (Figure 5.1 (c)) show no unusual feature on the surface whereas hill-like features can be observed in high quantities with denser clusters on sample stored in 100% RH for 14 days (Figure 5.1 (d)). Further, features can be seen in more developed volcano-like state following RH levels and at 100% RH YHO layers almost cracked completely. Similar feature was reported before [3] which was attributed to the result of oxidation from capping layer and/or glass substrate itself. We can speculate from the perspective of our results that

the permeability of the mentioned aluminum capping might also be enough for more extensive environmental interaction. Further, features appear like a bottom up delamination or a pressure buildup damage rather than dissolving by water in the environment [66] which should be expected from top-down. However, even though the delamination was the result, bottom-up damage from the feature and the water itself being the source might indicate a reaction in the YHO resulting this *eruption*. Also, non-homogenous dispersion of these features can indicate not one, but several sub-phases might present in photochromic YHO [93] and interacting with water at different rates. On the other hand, feature formation can be delayed by depositing denser films hence preventing high rate of interaction since the bottom-up nature of the features indicate a bulk interaction rather than a film surface interaction. These denser films would ultimately have slower oxidation during bleaching [12] and can result much longer recovery times [24].

5.3 Conclusion

We have studied photochromic properties and surface morphology of YHO in atmosphere of different humidity. We show that storing the YHO in humidity environment results in reduction of the film contrast and eventual delamination riddled with eruptive features. Therefore, the storage and working environment as well as encapsulation is critically important for applications of the YHO films in windows.

5.4 Acknowledgements

The work has been performed within FRINATEK project 287545 funded by the Research Council of Norway.

6. APPLICATIONS

Photochromic rare-earth metal oxyhydrides are multi-functional materials and realization into applications was a natural progress through my thesis study. It can be considered fortunate to be able to work with such versatile and structurally flexible materials where my studies produced two considerable applications: stable photochromic integrated glass units (IGUs) that modulate their optical properties through the day and photocatalysis which can present novel answers to our complex problems in modern age.

Applications are still in their early development phase where many aspects still need to be studied and improved much further. In this section, experimental results for two different application areas were presented and showing a glimpse of how large the potential rare-earth metal oxyhydride materials represent.

6.1 Integrated Glass Units (IGUs)

IGU production is a natural next step for photochromic thin film development where the main goal is reducing carbon footprint of structures where IGUs placed by limiting input from sun passively. Photochromic materials photodarken only by light irradiation, requiring nothing else i.e., heat, voltage, or different gases, which makes them a truly smart window technology. However, several challenges prevented the wide-spread use of this technology so far, such as degradation, price, large number process steps or difficulties etc. Photochromic applications include organic materials [100,101] dominantly but inorganic compounds such as molybdenum oxide [102], tungsten oxide [103,104] or silver halides [105] are also being developed. In 2011 [2], photochromic rare-earth metal oxyhydrides are also joined the photochromic family synthesized by two step process; reactively magnetron sputtering of a single rare-earth metal hydride layer and consecutive oxidation by air in seconds.

Investigation of photochromic rare-earth oxyhydrides gained momentum, which was explained in earlier part of this thesis, but production of rare-earth oxyhydride IGUs

was delayed because the lack of understanding of producing stable layers under air which also can modulate optical properties in a sensible time. As a result of this thesis study, stable photochromic yttrium oxyhydride IGUs are produced and currently long-term tests are underway. Initially, IGUs were produced with photochromic kinetics of 1:1 darkening/bleaching ratios (Figure 6.1) under illumination of AM1.5G Wavelabs Solar Simulator with 100% intensity. Later, it become possible to produce IGUs with rapid darkening and large contrasts (Figure 6.2) or fast bleaching with >20% contrasts (Figure 6.3) by improving deposition and production steps.

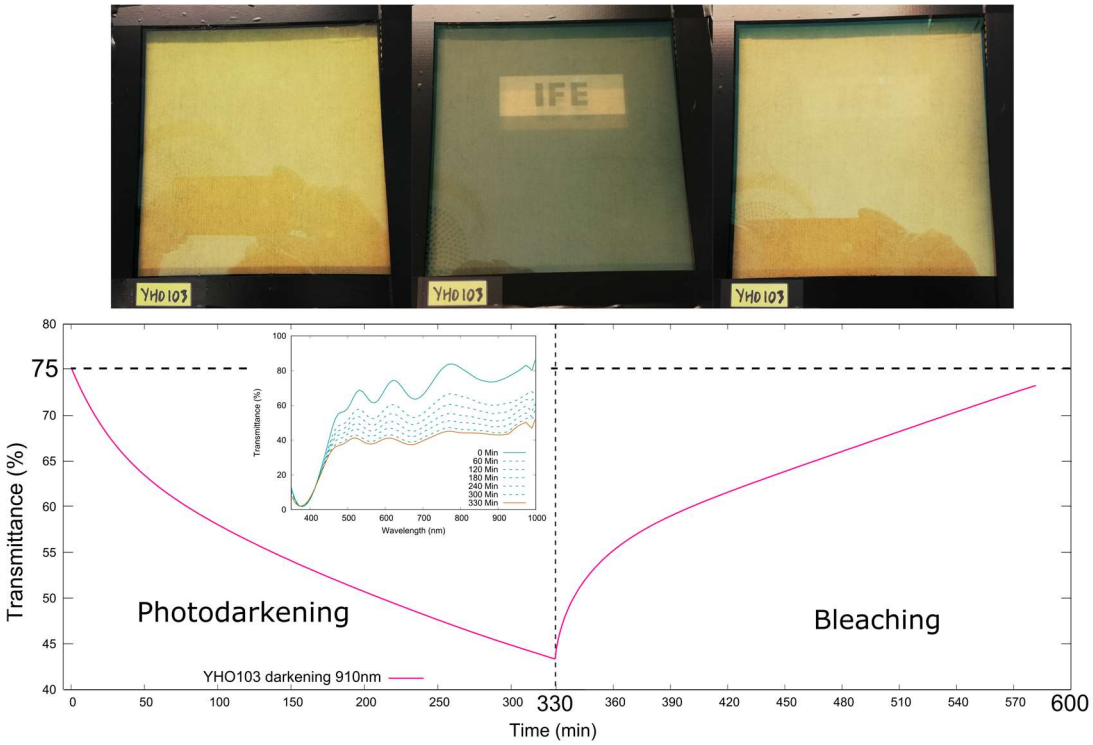

Figure 6.1 : Initial stable photochromic yttrium oxyhydride IGUs showing 30% contrast with 1:1 darkening/bleaching ratios.

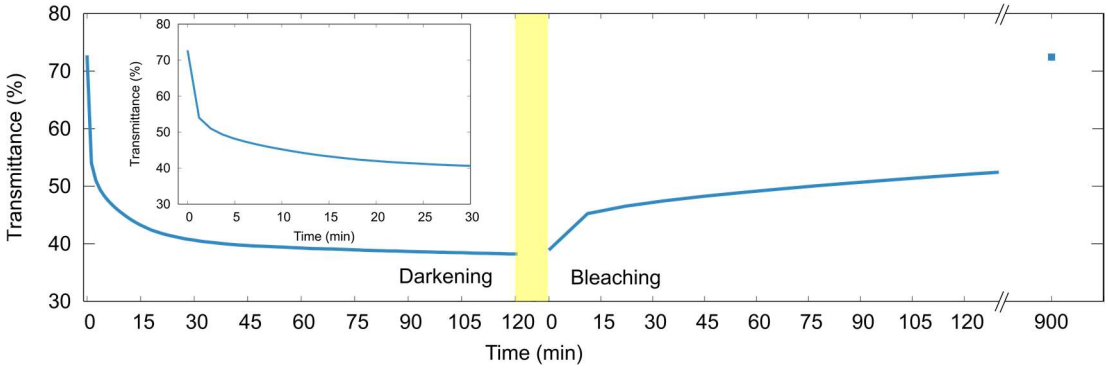

Figure 6.2 : Stable photochromic yttrium oxyhydride IGUs can be produced with >30% contrast with rapid darkening but requiring longer time for recovery.

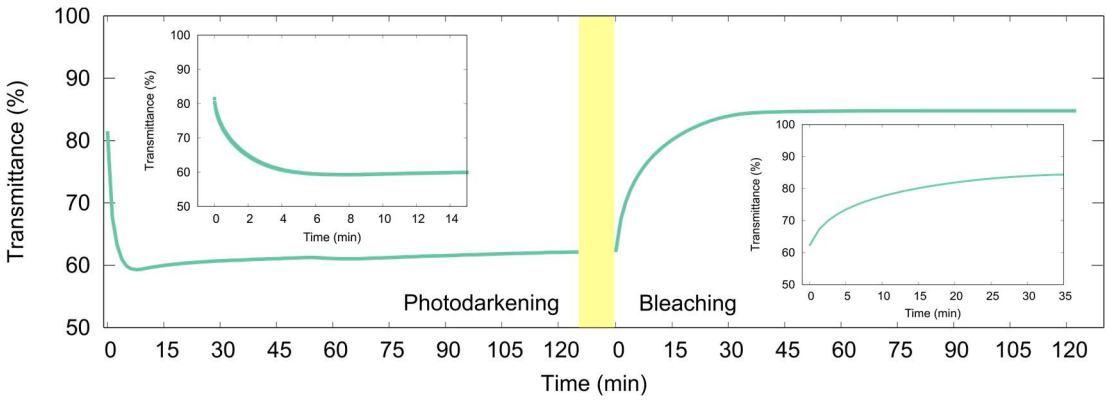

Figure 6.3 : Stable photochromic yttrium oxyhydride IGUs can be produced with rapid darkening (inlet, left top) and rapid bleaching (inlet, right bottom) with around >20% contrast.

Currently, rare-earth oxyhydride based IGU technology under development for even larger applications and considered to be a successful application. Through the know-how gathered during this thesis study, it is possible to produce photochromic rare-earth oxyhydride IGUs by other members of the rare-earth elements as well as yttrium and gadolinium.

6.2 Photocatalysis in GdHO

As deposited rare-earth metal hydrides transition into transparent insulator photochromic rare-earth oxyhydride following oxidation when exposed to air [3,28]. This transition is not permanent [12]; when UV-illuminated the photochromic rare-earth oxyhydride photodarkens approaching its initial metallic configuration [12,17] while also reducing electrical resistivity by up to a factor of 100 [2] depending on illumination time and recovers back when stored in dark. This modulation has interesting application potentials in memory devices and optical sensors, but more interesting applications can be realized by studying electronic configuration during this UV-illumination.

First electronic study of yttrium oxyhydride was performed by Mongstad et. al., who reported work function of 4.76 eV through Kelvin probe measurement. Kelvin probe [106] is a non-contact non-destructive measurement method that measures work function by measuring contact potential difference (CPD). CPD measures the surface potential difference between surfaces of vibrating reference electrode and the sample where sample work function can be calculated. CPD changes are related to changes in the electron affinity, shift in the bulk Fermi level and the band bending due to surface

states [71]. In the case of photochromic rare-earth oxyhydrides, increased electron concentration can be related to increase in the CPD.

Work function measurements were performed for GdHO samples deposited between 1-2.8 Pa deposition pressures with fixed 1:10 H_2/Ar flow ratio and 1.33 W/cm^2 power density. Work function of samples at their clear state varied between 2.96 – 4.06 eV following deposition pressure increase where the sample deposited at the lowest deposition pressure showing the lower work function (Figure 6.4). It should be noted that, work function decrease trend following decrease in deposition pressure also in accordance with the photochromic contrast (Figure 3.2) and preferential orientation (Figure 3.1). Upon illumination, every sample demonstrated decrease in work function values possibly because of increased electron concentration by formation of diluted metallic domains [17] at photodarkened state. Due to the lower surface to volume ratio of thin films, it can be expected to have a higher efficiency from photochromic rare-earth oxyhydride powders which should be the next step in the future.

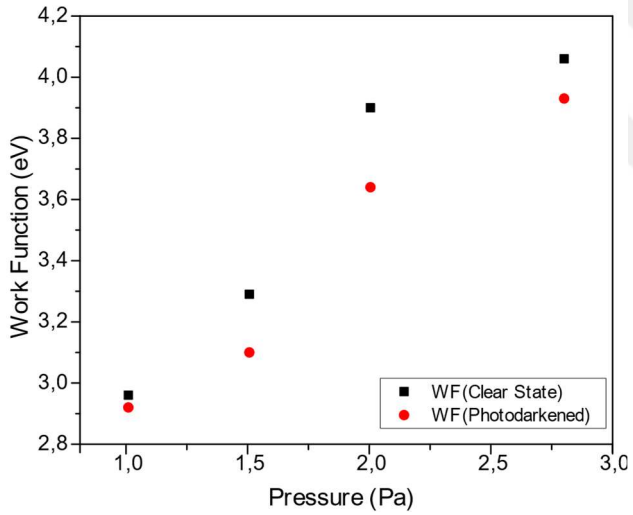

Figure 6.4 : Work function values of GdHO samples deposited between 1-2.8Pa deposition pressures. Work function of samples increases following deposition pressure increase. All samples show decrease in work function at photodarkened state after 30 minutes of UV illumination.

Decrease in work function values of GdHO samples under illumination led the study into photocatalytic investigation by methylene blue degradation efficiency under UV light illumination. It was found that each sample shows photocatalytic efficiency higher than 6% after 1 hours of illumination, increased to higher than 16% efficiency after 6 hours of illumination where the sample deposited under the lowest deposition pressure showing the highest efficiency throughout the experiment (Figure 6.5). This

efficiency and deposition pressure trend can be correlated with the higher electron concentration which was found by the work function measurements (Figure 6.4).

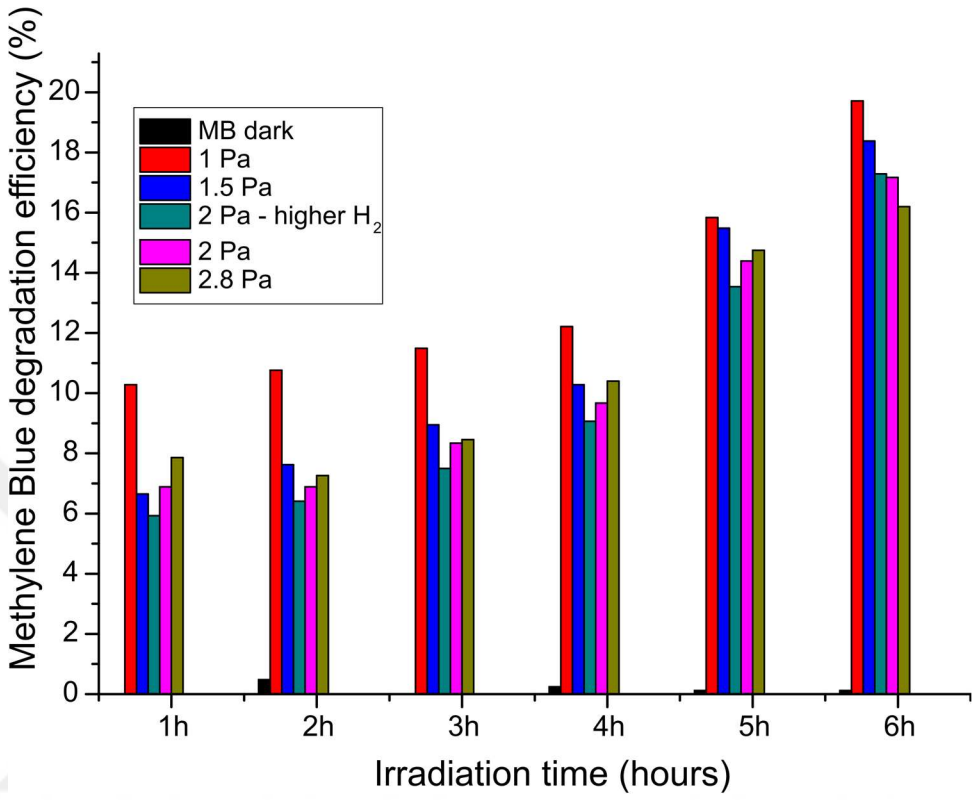

Figure 6.5 : Photocatalysis measurements of GdHO samples deposited between 1-2.8 Pa deposition pressures. Photocatalytic properties were measured by methylene blue degradation efficiency during 300W light irradiation (75% Vis, 25% UV) of the samples for 6 hours.

Photocatalytic materials present highly efficient and remarkable solutions for otherwise exceedingly difficult problems, i.e. surface self-cleaning [107], water purification [108], carbon dioxide conversion into fuels [109,110], photodegradation of contaminants [111] and especially hydrogen production by water splitting [112–114]. Applications in such areas will be one of the next most impactful steps into the future.

7. CONCLUSION

During this thesis study, the environmental effect on photochromic mechanism of rare-earth oxyhydrides using two members of the rare-earth elements, yttrium and gadolinium, has been investigated and results were published in three international journals. First, we have demonstrated that the oxidation during the synthesis of photochromic rare-earth oxyhydrides can, at least partially, be reverted by illumination; the YHO lattice contraction/expansion under illumination/darkness is accompanied by oxygen release/intake which causes the observed change in the optical properties, respectively. Further, we have subjected the YHO thin films to cyclic illumination under air and inert (N_2) atmospheres and revealed that the reversibility of the photochromic effect requires a source of oxygen in the environment. Also, we have found that the hydrophobic properties of the surface oxide layer have remarkably been enhanced by illumination with UV light. Contrary to well-known photoactive metal oxides, wettability of the surface has been reduced considerably because of the influence of UV illumination. XPS studies showed that, the reason of the enhancement of hydrophobicity is related to that of the increased oxygen content in the surface after UV illumination. Moreover, we have showed by theoretical modelling that the oxygen diffusion might be caused by the pseudo Jahn-Teller effect.

The study of the environment effect on the rare-earth metal oxyhydrides has been continued, by considering another member of the rare-earth metal oxyhydride class, gadolinium oxyhydride (GdHO), that has also been deposited by the reactive magnetron sputtering following the procedure established for the yttrium oxyhydride. We have found that the bandgap, photochromic performance, and structural properties can be controlled by deposition procedure and oxidation process. We have showed through chemical composition analysis using ToF ERDA that the higher deposition pressures result with higher oxygen content and lower photochromic contrast in GdHO films. Also, we found that one can control the preferential growth of GdHO films by controlling deposition process which also alters photochromic kinetics. For example, the higher orientation along the (200) direction resulted in higher photochromic contrasts. Controlling the bandgap by deposition parameter gives the key for the

materials engineering that can enhance flexibility in design, functionality, and possible applications.

Another study based on the interaction between environment and rare-earth metal oxyhydrides was also conducted within the thesis duration. We have investigated the delamination of yttrium oxyhydride thin films after illumination/darkness cycles or just by storing in air. We have found that the water in air causes the *volcano-like* micro features on yttrium oxyhydride thin films which results delamination from the substrate. Consequently, the formed features might indicate the interaction between water in air and the yttrium oxyhydride thin films is a bottom-up process, contrary to an etching effect. Also, it was found that the photochromic kinetics of yttrium oxyhydride thin films degrade heavily based on the humidity levels in the environment where the yttrium oxyhydride thin films stored. An article based on the destructive effect of water in air on yttrium oxyhydride thin films is under progress and expected to be submitted in an international article in 2021.

The initial aim at the beginning of this thesis, study of the environmental effect on rare-earth metal oxyhydrides, was satisfied by obtaining results and creating more questions by investigating effects of humidity, temperature, and oxidation in ambient conditions on yttrium oxyhydride and gadolinium oxyhydride. However, further studies are required to obtain a final answer for the photochromic mechanism question.

Motivated by the studies of influence of the environment on photochromic performance of the rare-earth metal oxyhydrides, we have investigated the influence of temperature of YHO thin films between 5-250K by Fourier transform infrared spectroscopy. Initially, YHO thin films were subjected to UV illumination/darkness cycle in ambient temperature and consecutively illuminated by UV at 5K. One of the theories suggested very recently for the photochromic process was the photon-induced hydrogen transfer between two different phases: from hydrogenated oxide phase to hydride phase. According to this theory, a photo-induced hydrogen transfer from hydrogenated oxide phase to hydride phase must occur to initiate photodarkening. One of the problems was the requirement of hydrogenation of oxide phase at ambient temperature during bleaching for rare-earth metal oxyhydride to have photochromic reversibility where rare-earth metal oxyhydride photochromic reversibility were demonstrated extensively in the literature. However, such a hydrogenation process for oxides is not possible at ambient temperature. Second problem was the irrefutable

dependency of the hydrogen transfer to the hydride phase. Instead, the results related to YHO films photodarkened at 5K suggest that either anion (hydride or oxide) out diffusion is not responsible for photodarkening since anion diffusion at 5K is too weak. It might, on the other hand, be the result of photon-induced bond breaking between anion(s) and yttrium and following charge transfer without any anion mobility. From the first study which YHO thin films were investigated under N_2 atmosphere and air, we concluded that the illumination with UV light has only broken the bond between yttrium and anion(s), however, anion(s) stayed in their sites at 5K. However, nuclear characterization studies can be a great approach to study anion mobility further after replacing anions of rare-earth metal oxyhydrides with their isotopes during synthesis. Following the remarkable photodarkening ability even at 5K, we studied the recovery of samples under darkness at 5K and as the temperature increased stepwise between 5-250K. Initially, we observed a very small recovery at 5K followed by additional small recovery until 100K. It was intriguing to observe any recovery below 100K because anion diffusion is substantially slowed down in such temperature range. For this reason, bleaching of the photodarkened films in this temperature range indicates to a possibility of strong contribution of electronic bleaching mechanism. It is possible that a charge transfer between two phases, opaque-metallic and transparent-semiconducting, can be responsible for this small bleaching effect which was demonstrated recently for MoO3:TiO2 crystalline-core amorphous-shell structures. Moreover, stronger recovery starting from 100K and above showed that the bleaching is a thermally driven process. Overall, the results showed that photochromic properties of YHO is based not only on anion diffusion.

Second aim of the thesis study, increasing the photochromic rare-earth metal oxyhydride knowledge in literature with another rare-earth element, fulfilled by the third published article based on gadolinium oxyhydride. Additional articles based on the gadolinium oxyhydride are in progress and expected to expand the knowledge even further.

During this thesis study, photochromic mechanism of rare-earth metal oxyhydrides were investigated with several approaches but, the photochromic mechanism has not been revealed yet. As the studies demonstrated, anion interaction and mobility hold a significant role for understanding the mechanism and measurement of anions in a mixed-anion material is not an easy task. One of the approaches in the future can be

made by replacing anions with their isotopes. Synthesis of rare-earth metal oxyhydride samples can be engineered by employing isotopes of hydrogen and oxygen which would allow the measurements with nuclear techniques as well as vibrational studies during the photodarkening/recovery more accessible and produce stronger signals for a better understanding. Also, studies of illumination source are still underdeveloped even tough there are reports showing the effect of different part of the spectrum on photochromic rare-earth metal oxyhydrides. Alternatively, it would be interesting to investigate higher power levels of irradiation sources (MW or GW levels) from different parts of the electromagnetic spectrum. Lastly, electronic properties of the rare-earth metal oxyhydrides require a better understanding and deserves a more intense focus. Photon-induced resistivity change was reported in literature and indicated photoconductive properties but investigation of this novel emerging class, mixed-anion rare-earth metal oxyhydrides, so far could only scratched the surface. Ultimately, considering the lack of information in conventional databases, there is potentially more room to discover that would result interesting applications.

During this thesis study, great deal of properties of mixed-anion photochromic rare-earth oxyhydride materials were discovered that can lead to exciting applications. One of such applications is the stable IGU development which was made into a product. IGUs that regulates the solar illumination passing through is a long-sought result which could not been realized into a product prior to this thesis study. Based on the results in this thesis, it became possible to develop a stable IGUs by YHO and GdHO.

The other application of oxyhydrides studied in the thesis is based on photocatalysis. We found that GdHO present photocatalytic properties, shown by methylene blue degradation under UV illumination up to 20% efficiency. It should be noted that the samples that had been tested were GdHO thin films and it is expected to observe increased efficiency by reducing the materials dimensions, i.e., nano size powders or nano-rods.

REFERENCES

[1] **Mongstad, T., Platzer-Björkman, C., Karazhanov, S.Z., Holt, A., Maehlen, J.P., Hauback, B.C.**, (2011). Transparent yttrium hydride thin films prepared by reactive sputtering, *J. Alloys Compd. 509***,** S812–S816.

[2] **Mongstad, T., Platzer-Björkman, C., Maehlen, J.P., Mooij, L.P.A., Pivak, Y., Dam, B… Karazhanov, S.Z.** (2011). A new thin film photochromic material: Oxygen-containing yttrium hydride, *Sol. Energy Mater. Sol. Cells*. *95,* 3596–3599.

[3] **Montero, J., Martinsen, F.A., Lelis, M., Karazhanov, S.Z., Hauback, B.C., Marstein, E.S.**, (2018). Preparation of yttrium hydride-based photochromic films by reactive magnetron sputtering, *Sol. Energy Mater. Sol. Cells*. *177,* 106–109.

[4] **Kantre, K., Moro, M. V., Moldarev, D., Wolff, M., Primetzhofer, D.**, (2020). Synthesis and in-situ characterization of photochromic yttrium oxyhydride grown by reactive e-beam evaporation, *Scr. Mater. 186,* 352–356.

[5] **Zapp, N., Auer, H., Kohlmann, H.**, (2019). YHO, an Air-Stable Ionic Hydride, *Inorg. Chem. 58,* 14635–14641.

[6] **Yamashita, H., Broux, T., Kobayashi, Y., Takeiri, F., Ubukata, H., Zhu, T… Kageyama, H.**, (2018). Chemical Pressure-Induced Anion Order-Disorder Transition in LnHO Enabled by Hydride Size Flexibility, *J. Am. Chem. Soc. 140,* 11170–11173.

[7] **Kageyama, H., Hayashi, K., Maeda, K., Attfield, J.P., Hiroi, Z., Rondinelli, J.M., Poeppelmeier, K.R.**, (2018). Expanding frontiers in materials chemistry and physics with multiple anions, *Nat. Commun. 9,* 772.

[8] **You, C.C., Karazhanov, S.Z.**, (2020). Effect of temperature and illumination conditions on the photochromic performance of yttrium oxyhydride thin films, *J. Appl. Phys. 128,* 013106.

[9] **Ohmura, A., MacHida, A., Watanuki, T., Aoki, K., Nakano, S., Takemura, K.**, (2007). Photochromism in yttrium hydride, *Appl. Phys. Lett. 91,* 151904.

[10] **Mongstad, T., Platzer-Björkman, C., Mæhlen, J.P., Hauback, B.C., Karazhanov, S.Z., Cousin, F.** (2012). Surface oxide on thin films of yttrium hydride studied by neutron reflectometry, *Appl. Phys. Lett. 100,* 1–4.

[11] **Maehlen, J.P., Mongstad, T.T., You, C.C., Karazhanov, S.** (2013). Lattice contraction in photochromic yttrium hydride, *J. Alloys Compd. 580*, S119–S121.

[12] **Baba, E.M., Montero, J., Strugovshchikov, E., Zayim, E.Ö., Karazhanov, S.** (2020). Light-induced breathing in photochromic yttrium oxyhydrides, *Phys. Rev. Mater. 4,* 1–8.

[13] **Hans, M., Tran, T.T., Aðalsteinsson, S.M., Moldarev, D., Moro, M. V., Wolff, M., Primetzhofer, D.** (2020). Photochromic Mechanism and Dual-Phase Formation in Oxygen-Containing Rare-Earth Hydride Thin Films, *Adv. Opt. Mater. 8,* 2000822.

[14] **Montero, J., Karazhanov, S.Z.** (2018). Spectroscopic Ellipsometry and Microstructure Characterization of Photochromic Oxygen-Containing Yttrium Hydride Thin Films, *Phys. Status Solidi Appl. Mater. Sci. 215,* 1–7.

[15] **Huiberts, J.N., Griessen, R., Rector, J.H., Wijngaarden, R.J., Dekker, J.P., De Groot, D.G., Koeman, N.J.** (1996). Yttrium and lanthanum hydride films with switchable optical properties, *Nature*. *380,* 231–234.

[16] **Chandran, C.V., Schreuders, H., Dam, B., Janssen, J.W.G., Bart, J., Kentgens, A.P.M., Van Bentum, P.J.M.** (2014). Solid-state NMR studies of the photochromic effects of thin films of oxygen-containing yttrium hydride, *J. Phys. Chem. C*. *118,* 22935–22942.

[17] **Montero, J., Martinsen, F.A., García-Tecedor, M., Karazhanov, S.Z., Maestre, D., Hauback, B., Marstein, E.S.** (2017). Photochromic mechanism in oxygen-containing yttrium hydride thin films: An optical perspective, *Phys. Rev. B*. *95,* 1–4.

[18] **You, C.C., Mongstad, T., Maehlen, J.P., Karazhanov, S.** (2014). Engineering of the band gap and optical properties of thin films of yttrium hydride, *Appl. Phys. Lett. 105,* 1–5.

[19] **You, C.C., Moldarev, D., Mongstad, T., Primetzhofer, D., Wolff, M., Marstein, E.S., Karazhanov, S.Z.** (2017). Enhanced photochromic response in oxygen-containing yttrium hydride thin films transformed by an oxidation process, *Sol. Energy Mater. Sol. Cells*. *166,* 185–189.

[20] **Montero, J., Galeckas, A., Karazhanov, S.Z.** (2018). Photoluminescence Properties of Photochromic Yttrium Hydride Films Containing Oxygen, *Phys. Status Solidi Basic Res. 255,* 1–5.

[21] **Moldarev, D., Wolff, M., Baba, E.M., Moro, M.V., You, C.C., Primetzhofer, D., Karazhanov, S.Z.** (2020). Photochromic properties of yttrium oxyhydride thin films: Surface versus bulk effect, *Materialia*. *11,* 100706.

[22] **Hallaråker, R.S.** (2018). *Temperature-and irradiation-dependent properties of photochromic thin films of YH x:O*. (Master's thesis) Norwegian University of Life Sciences, Ås.

[23] **Maehlen, J.P.** (2012). Photochromic Films of Transparent Yttrium Hydride: Advances in Structural Studies, in: Int. *Symp. Met. Syst.* TERRSA, Kyoto, Japan.

[24] **Nafezarefi, F., Schreuders, H., Dam, B., Cornelius, S.** (2017). Photochromism of rare-earth metal-oxy-hydrides, *Appl. Phys. Lett. 111,* 1–5.

[25] **La, M., Li, N., Sha, R., Bao, S., Jin, P.** (2018). Excellent photochromic properties of an oxygen-containing yttrium hydride coated with tungsten oxide (YHx:O/WO3), *Scr. Mater. 142***,** 36–40.

[26] **Moldarev, D., Moro, M. V., You, C.C., Baba, E.M., Karazhanov, S.Z., Wolff, M., Primetzhofer, D.** (2018). Yttrium oxyhydrides for photochromic applications: Correlating composition and optical response, *Phys. Rev. Mater. 2,* 1–6.

[27] **Nafezarefi, F., Cornelius, S., Nijskens, J., Schreuders, H., Dam, B.** (2019). Effect of the addition of zirconium on the photochromic properties of yttrium oxy-hydride, *Sol. Energy Mater. Sol. Cells*. *200,* 3–8.

[28] **Cornelius, S., Colombi, G., Nafezarefi, F., Schreuders, H., Renéheller, R., Munnik, F., Dam, B.** (2019). Oxyhydride Nature of Rare-Earth-Based Photochromic Thin Films, *J. Phys. Chem. Lett*. *10,* 43.

[29] **Moldarev, D., Primetzhofer, D., You, C.C., Karazhanov, S.Z., Montero, J., Martinsen, F… Wolff, M.** (2018). Composition of photochromic oxygen-containing yttrium hydride films, *Sol. Energy Mater. Sol. Cells*. *177,* 66–69.

[30] **Pishtshev, A., Karazhanov, S.Z.** (2014). Role of oxygen in materials properties of yttrium trihydride, *Solid State Commun. 194*, 39–42.

[31] **Baba, E.M., Montero, J., Moldarev, D., Moro, M.V., Wolff, M., Primetzhofer, D… Karazhanov, S.** (2020). Preferential Orientation of Photochromic Gadolinium Oxyhydride Films, *Molecules*. 25, 3181.

[32] **Baba, E.M., Weiser, P.M., Zayim, E.Ö.** (2020). Temperature-Dependent Photochromic Performance of Yttrium Oxyhydride Thin Films, *Phys. Status Solidi Rapid Res. Lett. 15*, 2000459.

[33] **Miniotas, A., Hjorvarsson, B., Douysset, L., Nostell, P.** (2000). Gigantic resistivity and band gap changes in GdOyHx thin films, *Appl. Phys. Lett. 76,* 2056–2058.

[34] **Kobayashi, Y., Hernandez, O., Tassel, C., Kageyama, H.** (2017). New chemistry of transition metal oxyhydrides, *Sci. Technol. Adv. Mater.*

18, 905–918.

[35] **Kobayashi, Y., Tsujimoto, Y., Kageyama, H.** (2018). Property Engineering in Perovskites via Modification of Anion Chemistry, *Annu. Rev. Mater. Res. 48,* 303–326.

[36] **Towns, A.D.** (2016). Industrial Photochromism, In Bergamini, G., Silvi, S. (Eds.) *Applied Photochemistry When Light Meets Molecules*, Springer International Publishing, Switzerland. (Vol.1 , pp. 227–279).

[37] **Zhang, Q., Xie, L., Zhu, Y., Tao, Y., Li, R., Xu, J… Jin, P.** (2019). Photo-thermochromic properties of oxygen-containing yttrium hydride and tungsten oxide composite films, *Sol. Energy Mater. Sol. Cells*. *200,* 109930.

[38] **Zenkin, S., Kos, Š., Musil, J.** (2014). Hydrophobicity of Thin Films of Compounds of Low-Electronegativity Metals, *J. Am. Ceram. Soc. 97,* 2713–2717.

[39] **Azimi, G., Dhiman, R., Kwon, H.M., Paxson, A.T., Varanasi, K.K.** (2013). Hydrophobicity of rare-earth oxide ceramics, *Nat. Mater. 12,* 315–320.

[40] **Ho, S.L., Kwak, D., Dong, Y.L., Seung, G.L., Cho, K.** (2007). UV-driven reversible switching of a roselike vanadium oxide film between superhydrophobicity and superhydrophilicity, *J. Am. Chem. Soc. 129,* 4128–4129.

[41] **Feng, X., Feng, L., Jin, M., Zhai, J., Jiang, L., Zhu, D.** (2004). Reversible Super-hydrophobicity to Super-hydrophilicity Transition of Aligned ZnO Nanorod Films, *J. Am. Chem. Soc. 126,* 62–63.

[42] **Yadav, K., Mehta, B.R., Bhattacharya, S., Singh, J.P.** (2016). A fast and effective approach for reversible wetting-dewetting transitions on ZnO nanowires, *Sci. Rep. 6,* 35073.

[43] **van Oss, C.J., Chaudhury, M.K., Good, R.J.** (1988). Interfacial Lifshitz—van der Waals and Polar Interactions in Macroscopic Systems, *Chem. Rev. 88,* 927–941.

[44] **van Oss, C.J.** (1993). Acid—base interfacial interactions in aqueous media, *Colloids Surfaces A Physicochem. Eng. Asp. 78,* 1-49.

[45] **Kresse, G., Furthmüller, J.** (1996). Efficient iterative schemes for ab initio total-energy calculations using a plane-wave basis set, *Phys. Rev. B - Condens. Matter Mater. Phys. 54,* 11169–11186.

[46] **Kresse, G., Furthmüller, J.** (1996). Efficiency of ab-initio total energy calculations for metals and semiconductors using a plane-wave basis set, *Comput. Mater. Sci. 6,* 15–50.

[47] **Kresse, G., Hafner, J.** (1994). *Ab initio* molecular-dynamics simulation of the liquid-metal–amorphous-semiconductor transition in germanium, *Phys. Rev. B*. *49,* 14251–14269.

[48] **Blöchl, P.E.** (1994). Projector augmented-wave method, *Phys. Rev. B*. *50,* 17953–17979.

[49] **Kresse, G., Joubert, D.** (1999). From ultrasoft pseudopotentials to the projector augmented-wave method, *Phys. Rev. B*. *59,* 1758–1775.

[50] **Kresse, G., Hafner, J.** (1993). Ab initio molecular dynamics for liquid metals, *Phys. Rev. B*. *47,* 558–561.

[51] **Perdew, J.P., Burke, K., Ernzerhof, M.** (1996). Generalized Gradient Approximation Made Simple, *Phys. Rev. Lett. 77,* 3865–3868.

[52] **Heyd, J., Scuseria, G.E., Ernzerhof, M.** (2003). Hybrid functionals based on a screened Coulomb potential, *J. Chem. Phys. 118,* 8207–8215.

[53] **Krukau, A. V., Vydrov, O.A., Izmaylov, A.F., Scuseria, G.E.** (2006). Influence of the exchange screening parameter on the performance of screened hybrid functionals, *J. Chem. Phys. 125,* 224106.

[54] **Henderson, T.M., Paier, J., Scuseria, G.E.** (2011). Accurate treatment of solids with the HSE screened hybrid, *Phys. Status Solidi*. *248,* 767–774.

[55] **Li, S.Y., Niklasson, G.A., Granqvist, C.G.** (2010). Nanothermochromics: Calculations for VO2nanoparticles in dielectric hosts show much improved luminous transmittance and solar energy transmittance modulation, *J. Appl. Phys. 108,* 063525.

[56] **Imanaka, N.** (2004). 5. Physical and Chemical Properties of Rare Earth Oxides, In Adachi, G., Imanaka, N., Kang, Z. C. (Eds.). *Binary Rare Earth Oxides*, Springer, Dordrecht. (vol. 1, pp. 111–133).

[57] **Feng, X., Zhai, J., Jiang, L.** (2005). The fabrication and switchable superhydrophobicity of TiO2 nanorod films, *Angew. Chemie - Int. Ed. 44,* 5115–5118.

[58] **Wang, S., Feng, X., Yao, J., Jiang, L.** (2006). Controlling wettability and photochromism in a dual-responsive tungsten oxide film, *Angew. Chemie - Int. Ed. 45,* 1264–1267.

[59] **Zhu, W., Feng, X., Feng, L., Jiang, L.** (2006). UV-Manipulated wettability between superhydrophobicity and superhydrophilicity on a transparent and conductive SnO2 nanorod film, *Chem. Commun. 26,* 2753–2755.

[60] **Sun, R., Nakajima, A., Fujishima, A., Watanabe, T., Hashimoto, K.** (2001). Photoinduced Surface Wettability Conversion of ZnO and TiO2 Thin Films, *J. Phys. Chem. B*. *105,* 1984–1990.

[61] **Kung, H.H.** (1991). Transition metal oxides: surface chemistry and catalysis. In *Advances in Colloid and Interface Science*. (pp. 53-71) .

[62] **Khan, S., Azimi, G., Yildiz, B., Varanasi, K.K.** (2015). Role of surface oxygen-to-metal ratio on the wettability of rare-earth oxides, *Appl. Phys. Lett. 106,* 061601.

[63] **Yumitori, S.** (2000). Correlation of C1s chemical state intensities with the O1s intensity in the XPS analysis of anodically oxidized glass-like carbon samples, *J. Mater. Sci. 35,* 139-146.

[64] **Preston, D.J., Miljkovic, N., Sack, J., Enright, R., Queeney, J., Wang, E.N.** (2014). Effect of hydrocarbon adsorption on the wettability of rare earth oxide ceramics, *Appl. Phys. Lett. 105,* 011601.

[65] **Lundy, R., Byrne, C., Bogan, J., Nolan, K., Collins, M.N., Dalton, E., Enright, R.** (2017). Exploring the Role of Adsorption and Surface State on the Hydrophobicity of Rare Earth Oxides, *ACS Appl. Mater. Interfaces*. *9,* 13751–13760.

[66] **Külah, E., Marot, L., Steiner, R., Romanyuk, A., Jung, T.A., Wäckerlin, A., Meyer, E.** (2017). Surface chemistry of rare-earth oxide surfaces at ambient conditions: Reactions with water and hydrocarbons, *Sci. Rep. 7,* 1–10.

[67] **Evans, S.** (1997). Correction for the effects of adventitious carbon overlayers in quantitative XPS analysis, *Surf. Interface Anal. 25,* 924-930.

[68] **Craciun, V., Howard, J., Lambers, E.S., Singh, R.K., Craciun, D., Perriere, J.** (1999). Low-temperature growth of Y2O3 thin films by Ultraviolet-Assisted Pulsed Laser Deposition, *Appl. Phys. A Mater. Sci. Process. 69,* S535-S538.

[69] **Tellez-Cruz, M.M., Padilla-Islas, M.A., Godínez-Salomón, J.F., Lartundo-Rojas, L., Solorza-Feria, O.** (2016). Y-OH-decorated-Pt/C electrocatalyst for oxygen reduction reaction, *Int. J. Hydrogen Energy*. *41,* 23318–23328.

[70] **Fujimori, A., Schlapbach, L.** (1984). Electronic structure of yttrium hydride studied by X-ray photoemission spectroscopy, *J. Phys. C Solid State Phys. 17*, 341.

[71] **Mongstad, T., Thøgersen, A., Subrahmanyam, A., Karazhanov, S.** (2014). The electronic state of thin films of yttrium, yttrium hydrides and yttrium oxide, *Sol. Energy Mater. Sol. Cells*. *128***,** 270–274.

[72] **Barshilia, H.C., Chaudhary, A., Kumar, P., Manikandanath, N.T.** (2012). Wettability of Y_2O_3: A Relative Analysis of Thermally Oxidized, Reactively Sputtered and Template Assisted Nanostructured Coatings., *Nanomater. (Basel, Switzerland)*. *2,* 65–78.

[73] **Ånes, H.W.** (2017). *Characterisation of photochromic oxygen-containing yttrium hydride by electron microscopy.* (Master's thesis) Norwegian University of Science and Technology, Trondheim.

[74] **Pishtshev, A., Strugovshchikov, E., Karazhanov, S.** (2018). Theoretical design of yttrium oxyhydrides : Remarkable richness of phase diagram. *ChemRxiv.* Available online: August 10 2018. https://doi.org/10.26434/chemrxiv.6950138.v1.

[75] **Bersuker, I.B.** (2013). Pseudo-Jahn-teller effect - A two-state paradigm in formation, deformation, and transformation of molecular systems and solids, *Chem. Rev. 113,* 1351–1390.

[76] **Widerøe, M., Fjellvåg, H., Norby, T., Willy Poulsen, F., Willestofte Berg, R.** (2011). NdHO, a novel oxyhydride, *J. Solid State Chem. 184,* 1890–1894.

[77] **Moro, M.V., Moldarev, D., You, C.C., Baba, E.M., Karazhanov, S.Z., Wolff, M., Primetzhofer, D.** (2019). In-situ composition analysis of photochromic yttrium oxy-hydride thin films under light illumination, *Sol. Energy Mater. Sol. Cells*. *201***,** 110119.

[78] **Plokker, M.P., Eijt, S.W.H., Naziris, F., Schut, H., Nafezarefi, F., Schreuders, H., Cornelius, S., Dam, B.** (2018). Electronic structure and vacancy formation in photochromic yttrium oxy-hydride thin films studied by positron annihilation, *Sol. Energy Mater. Sol. Cells*. *177***,** 97–105.

[79] **Eijt, S.W.H., De Krom, T.W.H., Chaykinab, D., Schut, H., Colombi, G., Cornelius, S… Dam, B.** (2020). Photochromic YOxHy thin films examined by in situ positron annihilation spectroscopy, *Acta Phys. Pol. A*. *137***,** 205–208.

[80] **You, C.C., Mongstad, T., Maehlen, J.P., Karazhanov, S.** (2015). Dynamic reactive sputtering of photochromic yttrium hydride thin films, *Sol. Energy Mater. Sol. Cells*. *143,* 623–626.

[81] **Petrov, I., Barna, P.B., Hultman, L., Greene, J.E.** (2003). Microstructural evolution during film growth, *J. Vac. Sci. Technol. A Vacuum, Surfaces, Film. 21,* S117–S128.

[82] **Anders, A.** (2010). A structure zone diagram including plasma-based deposition and ion etching, *Thin Solid Films*. *518,* 4087–4090.

[83] **Granqvist, C.G.** (1995). Tungsten Oxide Films: Preparation, Structure, and Composition of Sputter-Deposited Films. In Granqvist, C. G. (Ed.), *Handbook of Inorganic Electrochromic Materials* (1st ed., pp. 55-63) Elsevier, Amsterdam, The Netherlands.

[84] **Motohiro, T.** (2012). Computer Simulation In Handbook of Sputter Deposition Technology: Fundamentals and Applications for Functional Thin

Films, Nano-Materials and MEMS, (2nd ed., pp. 143-294) Elsevier Inc.

[85] **Montero, J., Guillén, C., Granqvist, C.G., Herrero, J., Niklasson, G.A.** (2014). Preferential Orientation and Surface Oxidation Control in Reactively Sputter Deposited Nanocrystalline SnO 2 :Sb Films: Electrochemical and Optical Results , *ECS J. Solid State Sci. Technol. 3,* N151–N153.

[86] **Van Steenberge, S., Leroy, W.P., Depla, D.** (2014). Influence of oxygen flow and film thickness on the texture and microstructure of sputtered ceria thin films, *Thin Solid Films*. *553,* 2–6.

[87] **Scherrer, P.** (1918). Bestimmung der größe und der inneren struktur von kolloidteilchen mittels röntgenstrahlen [Determination of the size and internal structure of colloidal particles using X-rays], *Nachr Ges Wiss Goettingen, Math-Phys Kl. 2,* 98–100.

[88] **Hong, S., Kim, E., Kim, D.W., Sung, T.H., No, K.** (1997). On measurement of optical band gap of chromium oxide films containing both amorphous and crystalline phases, *J. Non. Cryst. Solids*. *221,* 245–254.

[89] **Tauc, J.** (1974). Optical Properties of Amorphous Semiconductors. In Amorphous and Liquid Semiconductors. (1st ed. pp. 159-220) Springer US, Boston, MA.

[90] **Ström, P., Petersson, P., Rubel, M., Possnert, G.** (2016). A combined segmented anode gas ionization chamber and time-of-flight detector for heavy ion elastic recoil detection analysis, *Rev. Sci. Instrum. 87,* 103303.

[91] **Thornton, J.A.** (1977). High Rate Thick Film Growth, *Annu. Rev. Mater. Sci. 7,* 239–260.

[92] **Adachi, G.Y., Imanaka, N.** (1998). The binary rare earth oxides, *Chem. Rev. 98,* 1479–1514.

[93] **Pishtshev, A., Strugovshchikov, E., Karazhanov, S.** (2019). Conceptual Design of Yttrium Oxyhydrides: Phase Diagram, Structure, and Properties, *Cryst. Growth Des. 19,* 2574–2582.

[94] **Majer, G., Kaess, U., Barnes, R.G.** (1999). Model-independent measurements of hydrogen diffusivity in the lanthanum dihydride-trihydride system, *Phys. Rev. Lett. 83,* 340–343.

[95] **Shannon, R.D.** (1976). Revised effective ionic radii and systematic studies of interatomic distances in halides and chalcogenides, *Acta Crystallogr. Sect. A*. *32,* 751–767.

[96] **Li, N., Li, Y., Zhou, Y., Li, W., Ji, S., Yao, H… Jin, P.** (2017). Interfacial-charge-transfer-induced photochromism of MoO3@TiO2 crystalline-

core amorphous-shell nanorods, *Sol. Energy Mater. Sol. Cells*. *160,* 116–125.

[97] **Demiryont, H., Shannon, K.C.** (2007). Variable emittance electrochromic devices for satellite thermal control. In AIP Conference Proceedings, *880,* Albuquerque, New Mexico (USA).

[98] **Demiryont, H., Moorehead, D.** (2009). Electrochromic emissivity modulator for spacecraft thermal management, *Sol. Energy Mater. Sol. Cells*. *93,* 2075.

[99] **Greenspan, L.** (1977). Humidity Fixed Points of Binary Saturated Aqueous Solutions, *J Res Natl Bur Stand Sect A Phys Chem*. *81A,* 89–96.

[100] **Gentili, P.L., Micheau, J.C.** (2020). Light and chemical oscillations: Review and perspectives, *J. Photochem. Photobiol. C Photochem. Rev. 43,* 100321.

[101] **Towns, A.D.** (2016). Industrial Photochromism, In Bergamini, G., Silvi, S. (Eds.) Applied Photochemistry When Light Meets Molecules, Springer International Publishing, Switzerland. (Vol.1 , pp. 227–279).

[102] **Li, N., Li, Y., Sun, G., Zhou, Y., Ji, S., Yao, H… Jin, P.** (2017). Enhanced photochromic modulation efficiency: A novel plasmonic molybdenum oxide hybrid, *Nanoscale*. *9,* 8298–8304.

[103] **Popov, A.L., Han, B., Ermakov, A.M., Savintseva, I. V., Ermakova, O.N., Popova, N.R… Ivanov, V.K.** (2020). PVP-stabilized tungsten oxide nanoparticles: pH sensitive anti-cancer platform with high cytotoxicity, *Mater. Sci. Eng. C*. *108,* 110494.

[104] **Jiang, T., Guo, Z.** (2016). Robust superhydrophobic tungsten oxide coatings with photochromism and UV durability properties, *Appl. Surf. Sci. 387,* 412–418.

[105] **El-Zaiat, S.Y., Medhat, M., Omar, M.F., Shirif, M.A.** (2016). Effect of UV exposure on photochromic glasses doped with transition metal oxides, *Opt. Commun. 370,* 176–182.

[106] **Suresh Kumar, C., Subrahmanyam, A., Majhi, J.** (1996). Automated reed-type Kelvin probe for work function and surface photovoltage studies, *Rev. Sci. Instrum. 67,* 805–808.

[107] **Banerjee, S., Dionysiou, D.D., Pillai, S.C.** (2015). Self-cleaning applications of TiO2 by photo-induced hydrophilicity and photocatalysis, *Appl. Catal. B Environ. 176–177,* 396–428.

[108] **Riaz, S., Park, S.J.** (2020). An overview of TiO2-based photocatalytic membrane reactors for water and wastewater treatments, *J. Ind. Eng. Chem. 84,* 23–41.

[109] **Mazari, S.A., Hossain, N., Basirun, W.J., Mubarak, N.M., Abro, R., Sabzoi, N., Shah, A.** (2021). An overview of catalytic conversion of CO2 into fuels and chemicals using metal organic frameworks, *Process Saf. Environ. Prot. 149,* 67–92.

[110] **Dey, G.R.** (2007). Chemical Reduction of CO2 to Different Products during Photo Catalytic Reaction on TiO2 under Diverse Conditions: an Overview, *J. Nat. Gas Chem. 16,* 217–226.

[111] **Coelho, F.E.B., Gionco, C., Paganini, M.C., Calza, P., Magnacca, G.** (2019). Control of membrane fouling in organics filtration using Ce-doped Zirconia and visible light, *Nanomaterials*. *9(4),* 534.

[112] **Li, R.** (2017). Latest progress in hydrogen production from solar water splitting via photocatalysis, photoelectrochemical, and photovoltaic-photoelectrochemical solutions, *Cuihua Xuebao/Chinese J. Catal. 38,* 5–12.

[113] **Wang, Z., Fan, J., Cheng, B., Yu, J., Xu, J.** (2020). Nickel-based cocatalysts for photocatalysis: Hydrogen evolution, overall water splitting and CO2 reduction, *Mater. Today Phys. 18,* 100279.

[114] **Sun, X., Yuan, K., Zhang, Y.** (2020). Advances and prospects of rare earth metal-organic frameworks in catalytic applications, *J. Rare Earths*. *38,* 801–818.

CURRICULUM VITAE

Name Surname **:** Elbruz Murat Baba

Place and Date of Birth **:**

E-Mail **:**

EDUCATION **:**

- **M.Sc.** **:** 2015, Istanbul Technical University, Faculty of Nano Science and Nano Engineering, Department of Nano Science and Nano Engineering
- **B.Sc.** **:** 2012, Yıldız Technical University, Faculty of Naval Architecture and Maritime, Department of Naval Architecture and Marine Engineering

EXPERIENCE AND AWARDS:

- 2017 – present - Solar Cell Department, Institute for Energy Technology (IFE), Kjeller, Norway.
- 2017 August / 2018 June – University of Oslo - Erasmus student exchange programme
- 2015 October – 2016 October – Research Asistant - Şişecam Science and Technology Center - Atmospheric Depositions Department
- 100/2000 PhD Scholarship – Turkish Council of Higher Education (YÖK)

PUBLICATIONS AND PRESENTATIONS ON THE THESIS:

- **Baba E.M.,** Weiser P.M., Zayim E. and Karazhanov S. (2020). Temperature-Dependent Photochromic Performance of Yttrium Oxyhydride Thin Films, *Phys. Status Solidi RRL 2020, 2000459, 1-5.*
- **Baba E.M.,** Montero J., Moldarev D., Moro M.V., Wolff M., Primetzhofer D., Sartori S., Zayim E. and Karazhanov S. (2020). Preferential Orientation of Photochromic Gadolinium Oxyhydride Films, *Molecules*, 25, 3181.

- **Baba E.M.,** Montero J., Strugovshchikov E., Zayim E.Ö. and Karazhanov S. (2020). Light-Induced Breathing in Photochromic Yttrium Oxyhydrides, *Physical Review Materials,* 4, 025201.
- **Baba E.M.,** Moldarev D., Wolff M., Primetzhofer D., Cremades A., Taleno M., Montero J., Zayim E.Ö., and Karazhanov S. 2019: The European Materials Research Society (*E-MRS 2019*) Fall – International Congress – Band Gap, Optical and Compositional Engineering of Photochromic Gadolinium Oxy-Hydride Thin Films, September 16-19, 2019 Warsaw, Poland. Oral Presentation

OTHER PUBLICATIONS AND PRESENTATIONS:

- ICCE 21st International Conference on Composites or Nano Engineering 2013 "The Relationship Between Hydrophobicity and Transmittance Properties of Polyolefin/Inorganic Oxide Surfaces" Oral Presentation
- SATF Science & Application of Thin Films, Conference & Exhibition 2014 "Dependence of Optical and Mechanical Properties on Wettabilities And Surface Free Energies of The Polymers" Poster Presentation
- ECASIA 16th European Conference on Applications of Surface and Interface Analysis 2015 "Investigation of Optical and Wettability Properties of Polystyrene-SiO_2 Nanoparticle Composite Films" September28-October 01.
- **Baba E.M.,** Cansoy C.E., Zayim E.Ö. **(**2016). Investigation of Optical and Wettability Properties of Polystyrene-SiO_2 Nanoparticle Composite Films, *Progress in Organic Coatings, 99*, 378-385.
- **Baba E.M.,** Cansoy C.E., Zayim E.Ö. **(**2015). Optical and Wettability Properties of Polymers with Varying Surface Energies, *Applied Surface Science, 350*, 115-120.